Response to reviewer comments:

The authors thank the reviewer for the comments that improve the quality of the paper. The reviewer comments are shown in italic fonts, the responses are in regular fonts, and revised text in bold fonts.

Thank you for the detailed response to reviewers' comments. I think you have addressed their comments sufficiently. I just have a few very minor technical notes. The manuscript will be accepted for publication in ACP once these are addressed.

(the line numbers correspond to those in the revised manuscript)

Comment 1: *Line 114. It would also be appropriate to cite Bean and Hildebrandt Ruiz (ACP, 2016), Boyd et al. (ACP, 2015), and Boyd et al. (ES&T, 2017).*

Response 1: We have added those citations in lines 107-111 of the revised paper as:
"**The fate of particle-phase RONO$_2$ is unclear, with the possibility for removal by hydrolysis to form HNO$_3$ (Jacobs et al., 2014; Hu et al., 2011; Darer et al., 2011; Rindelaub et al., 2015; Szmigielski et al., 2010; Sato, 2008; Romer et al., 2016; Wolfe et al., 2015; Boyd et al., 2017; Boyd et al., 2015; Bean and Hildebrandt Ruiz, 2016), ...**"

Comment 2. *Line 116. Delete citation of Boyd et al. in this sentence, as this work does not discuss photochemical aging.*

Response 2: That citation has been removed and the text is revised as:
"**...photochemical aging (Nah et al., 2016), ...**"

Comment 3. *Line 227. Also isoprene oxidation by NO$_3$? This was discussed in the next paragraph.*

Response 3: We agree with the reviewer. Now the text reads as (in lines 194-196):
"**This mechanism is based on Mao et al. (2013b), but has been significantly revised to incorporate recent laboratory updates on isoprene oxidation by OH, O$_3$ and NO$_3$ ....**"

Comment 4: *Line 287. A few recent laboratory studies have investigated the effects of RO2 fates on aerosol formation from nitrate radical oxidation, representative of different atmospheric environments (Ng et al., ACP, 2008; Boyd et al., ACP, 2015; Schwantes et al., J. Phys. Chem. A, 2015). More studies are needed definitely, especially regarding the role of RO2 autoxidation in nitrate radical oxidation chemistry.*

Response 4: Now the text reads as (in lines 244-248):

"**However, these results might not be representative of atmospheric conditions in terms of the RO$_2$ reaction partner or RO$_2$ lifetime, warranting further studies on the effects of RO$_2$ fates on aerosol formation (Boyd et al., 2017; Boyd et al., 2015; Ng et al., 2008; Schwantes et al., 2015).**"

Comment 5: *Line 306. I think the "hydro full" case does not include the hydrolysis of TERPN2 (monoterpene nitrates from NO3 oxidation)? It would be useful to state this here explicitly for clarity.*

Response 5: Hydrolysis of TERPN2 is not included in the "hydro_full" case. We have emphasized this in lines 262-264 as:

"**One is "hydro_full" case including heterogeneous loss of a C$_5$ dihydroxy dinitrate (DHDN) and monoterpene nitrates only from OH oxidation during daytime (TERPN1; nighttime monoterpene nitrates are excluded), ...**"

Decadal change of summertime reactive oxidized nitrogen and surface ozone over the Southeast United States

Jingyi Li[1], Jingqiu Mao[2], Arlene M. Fiore[3],Ronald C. Cohen[4,5], John D. Crounse[6], Alex P. Teng[6], Paul O. Wennberg[6,7], Ben H. Lee[8], Felipe D. Lopez-Hilfiker[8], Joel A. Thornton[8], Jeff Peischl[9,10], Ilana B. Pollack[11], Thomas B. Ryerson[9], Patrick Veres[9,10], James M. Roberts[9], J. Andrew Neuman[9,10], John B. Nowak[12,a], Glenn M. Wolfe[13,14], Thomas F. Hanisco[14], Alan Fried[15], Hanwant B. Singh[16], Jack Dibb[17], Fabien Paulot[18,19], Larry W. Horowitz[19]

[1]Jiangsu Key Laboratory of Atmospheric Environment Monitoring and Pollution Control, Collaborative Innovation Center of Atmospheric Environment and Equipment Technology, School of Environmental Science and Engineering, Nanjing University of Information Science and Technology, Nanjing, Jiangsu, 210044, China
[2]Department of Chemistry and Biochemistry & Geophysical Institute, University of Alaska Fairbanks, Fairbanks, Alaska, 99775, USA
[3]Department of Earth and Environmental Sciences & Lamont-Doherty Earth Observatory of Columbia University, Palisades, New York, 10027, USA
[4]Department of Chemistry, University of California, Berkeley, Berkeley, California, 94720, USA
[5]Department of Earth and Planetary Science, University of California, Berkeley, Berkeley, California, 94720, USA
[6]Division of Geological and Planetary Sciences, California Institute of Technology, Pasadena, California, 91125, USA
[7]Division of Engineering and Applied Science, California Institute of Technology, Pasadena, California, 91125, USA
[8]Department of Atmospheric Sciences, University of Washington, Seattle, Washington, 98195, USA
[9]Chemical Sciences Division, NOAA Earth System Research Laboratory, Boulder, Colorado, 80305, USA
[10]Cooperative Institute for Research in Environmental Science, University of Colorado Boulder, Boulder, Colorado, 80309, USA
[11]Department of Atmospheric Science, Colorado State University, Fort Collins, Colorado, 80523, USA
[12]Aerodyne Research, Inc., Billerica, Massachusetts, 01821, USA
[13]Joint Center for Earth System Technology, University of Maryland Baltimore County, Baltimore, Maryland, 21250, USA
[14]Atmospheric Chemistry and Dynamics Lab, NASA Goddard Space Flight Center, Greenbelt, Maryland, 20771, USA
[15]Institute of Arctic & Alpine Research, University of Colorado, Boulder, Colorado, 80309, USA
[16]NASA Ames Research Center, Moffett Field, California, 94035, USA
[17]Department of Earth Sciences and Institute for the Study of Earth, Oceans, and Space, University of New Hampshire, Durham, New Hampshire, 03824, USA
[18]Program in Atmospheric and Oceanic Sciences, Princeton University, Princeton, New Jersey, 08544, USA
[19]Geophysical Fluid Dynamics Laboratory/National Oceanic and Atmospheric Administration, Princeton, New Jersey, 08540, USA
[a]now at: NASA Langley Research Center, Hampton, Virginia, USA

Correspondence to: Jingqiu Mao (jmao2@alaska.edu)

Abstract

Widespread efforts to abate ozone (O_3) smog have significantly reduced nitrogen oxides (NO_x) emissions over the past two decades in the Southeast U.S. (SEUS), a place heavily influenced by both anthropogenic and biogenic emissions. How reactive nitrogen speciation responds to the reduction in NO_x emissions in this region remains to be elucidated. Here we exploit aircraft measurements from ICARTT (July-August, 2004), SENEX (June-July, 2013), and SEAC[4]RS (August-September, 2013) and long-term ground measurement networks alongside a global chemistry-climate model to examine decadal changes in summertime reactive oxidized nitrogen (RON) and ozone over the Southeast U.S. We show that our model can well reproduce the mean vertical profiles of major RON species and the total (NO_y) in both 2004 and 2013. Among the major RON species, nitric acid (HNO_3) is dominated (~ 42 – 45 %), followed by NO_x (31 %), total peroxy nitrates ($\sum$PNs; 14 %), and total alkyl nitrates ($\sum$ANs; 9 – 12 %) on a regional scale. We find that most RON, including NO_x, $\sum$PNs and HNO_3 decline proportionally with decreasing NO_x emissions in this region, leading to a similar decline in NO_y. This linear response might be in part due to the nearly constant summertime supply of biogenic VOC emissions in this region. Our model captures the observed relative change of RON and surface ozone from 2004 to 2013. Model sensitivity tests indicate that further reductions of NO_x emissions will lead to a continued decline in surface ozone and less frequent high ozone events.

1 Introduction

Since the 1990s, the U.S.A. Environmental Protection Agency (U.S. EPA) has targeted emissions of nitrogen oxides (NO_x) to improve air quality by lowering regional photochemical smog (The 1990 Clean Air Amendment). Satellite- and ground-based observations imply significant declines in U.S. NO_x emissions, with a decreasing rate of roughly - 4 % yr^{-1} after 2005 (Krotkov et al., 2016; Russell et al., 2012; Tong et al., 2015; Miyazaki et al., 2017; Lu et al., 2015; Lamsal et al., 2015). This has proven effective at lowering near-surface ozone (O_3) in the past few decades (Cooper et al., 2012; Simon et al., 2015; Hidy and Blanchard, 2015; Stoeckenius et al., 2015; Xing et al., 2015; Yahya et al., 2016; Astitha et al., 2017). The average of the annual 4th highest daily maximum 8-h average (MDA8) ozone over 206 sites has decreased by 31 % from 101 ppb in 1980 to 70 ppb in 2016 across the continental U.S., with more significant reductions in rural areas of the eastern U.S. in summer (Simon et al., 2015; Cooper et al., 2012). Here we use both aircraft and ground-based datasets, combined with a high resolution chemistry-climate model, to evaluate responses of reactive oxidized nitrogen (RON) and surface ozone to the NO_x emission reductions in the Southeast U.S.

In the troposphere, ozone is produced through photochemical reactions involving NO_x and volatile organic compounds (VOCs) in the presence of sunlight. During photooxidation, a large fraction of NO_x is transformed into its reservoirs, including nitric acid (HNO_3), peroxy nitrates (RO_2NO_2; dominated by peroxyacetyl nitrate (PAN)), and alkyl nitrates ($RONO_2$). These species, together with NO_x, are known as total reactive oxidized nitrogen ($NO_y = NO_x + HNO_3 + HONO$

81 + 2 × N$_2$O$_5$ + total peroxy nitrates ($\sum$PNs) + total alkyl nitrates ($\sum$ANs)). Some of these reservoir
82 species, particularly those with an organic component, tend to be less soluble and longer lived.
83 They may carry reactive nitrogen far from the NO$_x$ source region (Stohl et al., 2002; Parrish et al.,
84 2004; Li et al., 2004) and thereby affect NO$_x$ concentrations and O$_3$ formation on a regional to
85 global scale (Liang et al., 1998; Horowitz et al., 1998; Perring et al., 2013; Paulot et al., 2016;
86 Hudman et al., 2004).

87 RONO$_2$ originating from biogenic VOCs (BVOCs) represents a major uncertainty in the NO$_y$
88 budget, as BVOC emissions account for more than 80 % of global VOC emissions (Millet et al.,
89 2008). To a large extent, this is due to the uncertainties in current understanding of BVOC
90 oxidation chemistry. Biogenic RONO$_2$ species are mainly produced from the oxidation of
91 BVOCs by OH in the presence of NO$_x$ during daytime and by nitrate radical (NO$_3$) during
92 nighttime. Laboratory and field studies show a wide range of RONO$_2$ yields from their BVOC
93 precursors (Browne et al., 2014; Fry et al., 2014; Lockwood et al., 2010; Paulot et al., 2009;
94 Rindelaub et al., 2015; Rollins et al., 2009; Lee et al., 2014; Xiong et al., 2015; Xiong et al.,
95 2016; Teng et al., 2015). Another uncertainty lies in the fate of RONO$_2$, i.e. recycling RONO$_2$
96 into NO$_x$ or converting it to HNO$_3$ have important implications for the NO$_y$ budget and thus O$_3$
97 production (Fiore et al., 2005; Horowitz et al., 2007; Ito et al., 2009; Perring et al., 2013; Paulot
98 et al., 2012). This is further complicated by particle-phase RONO$_2$, an important component of
99 secondary organic aerosol (SOA) over the Southeast U.S. (Xu et al., 2015; Lee et al., 2016). The
100 fate of particle-phase RONO$_2$ is unclear, with the possibility for removal by hydrolysis to form
101 HNO$_3$ (Jacobs et al., 2014; Hu et al., 2011; Darer et al., 2011; Rindelaub et al., 2015; Szmigielski
102 et al., 2010; Sato, 2008; Romer et al., 2016; Wolfe et al., 2015; Boyd et al., 2017; Boyd et al.,
103 2015; Bean and Hildebrandt Ruiz, 2016), photochemical aging (Nah et al., 2016; Boyd et al.,
104 2015), and deposition (Nguyen et al., 2015).). To what extent RONO$_2$ affect the partitioning of
105 RON and surface ozone remains to be elucidated.

106 Extensive datasets in the Southeast U.S. offer a great opportunity to study the decadal change of
107 RON and surface ozone, resulting from NO$_x$ emission decline. Aircraft campaigns during the
108 summers of 2004 and 2013, including the International Consortium for Atmospheric Research on
109 Transport and Transformation (ICARTT) (Fehsenfeld et al., 2006; Singh et al., 2006), the
110 Southeast Nexus (SENEX) (Warneke et al., 2016), and the Studies of Emissions and
111 Atmospheric Composition, Clouds and Climate Coupling by Regional Surveys (SEAC[4]RS)
112 (Toon et al., 2016), provide detailed characterization of tropospheric composition in this region
113 separated by nearly a decade. These data have been widely used to evaluate model estimates of
114 RON and ozone (Singh et al., 2007; Pierce et al., 2007; Perring et al., 2009; Fischer et al., 2014;
115 Hudman et al., 2007; Henderson et al., 2011; Hudman et al., 2009; Edwards et al., 2017; Baker
116 and Woody, 2017; Travis et al., 2016; Mao et al., 2013b; Fisher et al., 2016; Yu et al., 2016; Liu
117 et al., 2016). Together with measurements from networks, including the National Atmospheric
118 Deposition Program (NADP) and EPA Air Quality System (AQS), these datasets enable a close
119 examination of responses of RON and surface ozone to NO$_x$ emissions reduction in this region.

120   Here we use a high-resolution global 3D climate-chemistry model, the Geophysical Fluid
121   Dynamics Laboratory (GFDL) AM3 model, with updated isoprene and organic nitrate chemistry
122   to investigate decadal changes of RON and surface O_3 during summer between 2004 and 2013
123   over the Southeast U.S. We first evaluate the model with comprehensive measurements from
124   three aircraft campaigns in the summer of 2004 (ICARTT) and 2013 (SENEX and SEAC[4]RS).
125   Model estimates of nitrate wet deposition flux are also evaluated against measurements from
126   NADP; model estimates of NO_y are compared with measurements from EPA AQS to provide an
127   additional constraint on the fate of RON in the model. We then investigate the repartitioning of
128   RON in response to NO_x emission reductions from 2004 to 2013 on a regional scale. From there,
129   we examine the model estimate of decadal changes of summertime surface O_3 at 157 EPA AQS
130   monitoring sites over the Southeast U.S. We also demonstrate the sensitivity of RON and MDA8
131   O_3 to a hypothetical NO_x emission reduction over the next decade.

132   2 Methodology

133   2.1 AM3 Model

134   We apply a high-resolution (50 x 50 km^2) version of the GFDL AM3 global chemistry-climate
135   model to study decadal changes of RON and O_3 over the Southeast U.S. Chemistry-climate
136   models provide a unique capability to both evaluate model representation of these observed
137   changes and use that to improve future projections of air quality in the same region. The model
138   configuration is to a large extent similar to that used in another paper (Li et al., 2016); and a
139   short summary is provided below. The dynamical core, physical parameterizations, cloud and
140   precipitation processes, and cloud-aerosol interactions mainly follow Donner et al. (2011),
141   except that convective plumes are computed on a vertical grid with finer resolution (Paulot et al.,
142   2016). Dry deposition in the model has been updated to use dry deposition velocities calculated
143   in the GEOS-Chem model (Paulot et al., 2016), to reflect rapid deposition of organic nitrates and
144   oxidized volatile organic compounds (OVOCs) (Nguyen et al., 2015). The current time step for
145   chemistry and transport in our model is 20 mins. We show below in section 4.1 that, with the
146   current setting, our model can well reproduce the vertical profiles of RON. Sensitivity of RON to
147   operator duration should refer to Philip et al. (2016).

148   Isoprene emissions are computed in the model using the Model of Emissions of Gases and
149   Aerosols from Nature (MEGAN). In 2004, isoprene emissions over the continental U.S. (25-50°
150   N, 130-70° W) are computed to be 8.0 Tg C in July and August together, with a previous model
151   estimate of 7.5 Tg C by Mao et al. (2013b). In 2013, model estimates of isoprene emissions were
152   scaled down by 20% following Li et al. (2016). The resulting isoprene emissions are 7.7 Tg C in
153   July-August in this region, with little difference compared to 2004. Monoterpene emissions
154   follow Naik et al. (2013) and do not vary interannually, with a total of 4.0 Tg C in July and
155   August.

156 Anthropogenic emissions follow the Representative Concentration Pathway 8.5 (RCP 8.5)
157 projection (Lamarque et al., 2011) for both 2004 and 2013, to compare the model to observations
158 in a consistent fashion and also enable future projection of air quality in this region. As shown in
159 Table 1, anthropogenic NO_x emissions over the continental U.S. during July-August of 2004
160 amount to 0.42 Tg N mon^{-1}, consistent with Hudman et al. (2007) but 11 % lower than EPA
161 estimates of 0.47 Tg N mon^{-1} (Granier et al., 2011). For the year of 2013, we apply a 25 %
162 reduction to the anthropogenic NO_x emissions from the RCP 8.5 projection (from base year of
163 2010), to best reproduce the vertical profiles of RON during SENEX as shown below in section
164 4.1. This adjustment is also consistent with recent estimates of NO_x emissions over the Southeast
165 U.S. (Anderson et al., 2014). The resulting anthropogenic NO_x emissions (0.25 Tg N mon^{-1}) are
166 14 % lower than NEI11v1 emission inventory estimate of 0.29 Tg N mon^{-1} (0.28 Tg N mon^{-1}
167 from the updated NEI11v2 emission inventory), although both inventories have a similar spatial
168 distribution (Figure S1). We also apply a diurnal variation to anthropogenic NO_x emissions
169 following Mao et al. (2013b). Soil NO_x emissions in our model, 3.6 Tg N yr^{-1} globally (Naik et
170 al., 2013), are considerably lower than other model estimates, including 5.5 Tg N yr^{-1} in Yienger
171 and Levy (1995) and 9.0 Tg N yr^{-1} in Hudman et al. (2012). As a result, the anthropogenic NO_x
172 emissions over the continental U.S. are 0.84 Tg N for July-August of 2004, and 0.50 Tg N in
173 July-August of 2013, with 40 % reduction from 2004 to 2013 (Table 1). This relative change in
174 anthropogenic NO_x emissions is consistent with EPA estimates (https://www.epa.gov/air-
175 emissions-inventories/air-pollutant-emissions-trends-data) and satellite observations (Krotkov et
176 al., 2016; Lu et al., 2015). Compared to the NEI11v1 inventory, RCP 8.5 used in our model
177 shows similar relative differences in both national and Southeast region.

2.2 Gas-phase chemistry

179 We apply the same isoprene mechanism as described by Li et al. (2016). A full list of the
180 reactions can be found in Table S1. This mechanism is based on Mao et al. (2013b), but has been
181 significantly revised to incorporate recent laboratory updates on isoprene oxidation by OH, O_3
182 and $NO_3$$O_3$ (Schwantes et al., 2015; Bates et al., 2016; Peeters et al., 2014; St. Clair et al., 2016;
183 Bates et al., 2014; Praske et al., 2015; Müller et al., 2014; Lee et al., 2014; Crounse et al., 2011).
184 One major feature is the suppression of δ-isoprene hydroxyl peroxy radical (δ-ISOPO$_2$) and
185 subsequent reaction pathways in the model, as these channels are considered to be of minor
186 importance under ambient conditions (Peeters et al., 2014; Bates et al., 2014). The fraction of
187 ISOPO$_2$ undergoing isomerization is calculated using bulk isomerization estimates (Crounse et
188 al., 2011). As a result, the first-generation isoprene alkyl nitrate is assumed to be β-hydroxy
189 nitrate (ISOPNB) in the model with a yield of 10 % from the ISOPO$_2$ + NO pathway. This
190 differs from a recent GEOS-Chem study of organic nitrates over the Southeast U.S. that assumed
191 9 % yield of the first-generation isoprene alkyl nitrate comprised of 90 % ISOPNB and 10 % δ-
192 hydroxy nitrate (ISOPND) (Fisher et al., 2016). The treatment of β- and δ-ISOPO$_2$ will not only
193 affect the speciation of organic nitrates but also the production of O$_3$ due to different NO_x
194 recycling efficiency in their secondary products. We also include updated chemistry for

methylvinyl ketone (MVK) (Praske et al., 2015), an updated yield of hydroxy hydroperoxides (ISOPOOH) (Bates et al., 2016; St. Clair et al., 2016), fast photolysis of carbonyl organic nitrates (Müller et al., 2014), and an updated ozonolysis rate of ISOPNB (Lee et al., 2014). In addition, we reduce the yield of organic nitrates (MACRN) from methacrolein (MACR) oxidation from 15 % to 3 %, which is estimated from the measured yield of nitrate from MVK oxidation (Praske et al., 2015).

Another major model revision involves the treatment of nighttime oxidation of isoprene. Instead of following Mao et al. (2013b), we revised nighttime oxidation of isoprene largely based on the Leeds Master Chemical Mechanism v3.2 (MCM v3.2), allowing a more complete description of isoprene oxidation by NO_3. In particular, MCM v3.2 suggests significant production of propanone nitrate (PROPNN) from the photooxidation of the C_5 carbonyl nitrate, consistent with recent laboratory experiments (Schwantes et al., 2015). We also updated the products of the reaction of nitrooxy alkylperoxy radical (INO$_2$), the peroxy radical from isoprene oxidation by NO_3, with HO_2 to reflect a lower molar yield (0.77) of C_5 nitrooxy hydroperoxide (INPN) (Schwantes et al., 2015). The differences between MCM v3.2 and the most updated version, MCM v3.3.1, in isoprene nighttime chemistry appears to be small (Jenkin et al., 2015). We therefore use MCM v3.2 as the reference in this work.

We include a highly simplified chemistry for the oxidation of monoterpenes in this work, mainly to quantify their contribution to organic nitrates. Monoterpenes are lumped into one chemical species ($C_{10}H_{16}$) in our model. The organic nitrate yield is set to 26 % from OH-initiated oxidation (Rindelaub et al., 2015) and to 10 % from NO_3-initiated oxidation (Browne et al., 2014). Details of the monoterpene chemistry can be found in Table S2.

2.3 Heterogeneous loss of organic nitrates

Field and laboratory studies have indicated a potential contribution to aerosol formation of organic nitrates from BVOC oxidation (Ayres et al., 2015; Fry et al., 2014; Nah et al., 2016; Rollins et al., 2009; Rindelaub et al., 2015; Boyd et al., 2015; Lee et al., 2016; Ng et al., 2008; Fry et al., 2009; Xu et al., 2015; Lee et al., 2014; Bean and Hildebrandt Ruiz, 2016; Spittler et al., 2006; Boyd et al., 2017).). Aerosol yield depends on both the VOC precursor and the oxidant. For example, Δ-3-carene oxidation by NO_3 can produce a 38-65 % yield of organic aerosols in a smog chamber (Fry et al., 2014), which is much higher than the 1-24 % yield from NO_3-initiated isoprene oxidation (Ng et al., 2008; Rollins et al., 2009; Ayres et al., 2015). Recent chamber studies indicate a very low aerosol yield from α-pinene oxidation by NO_3 (Nah et al., 2016; Fry et al., 2014), the aerosol yield increases to ~ 18 % when α-pinene is oxidized by OH (Rollins et al., 2010; Rindelaub et al., 2015). However,It should be noted that these results from laboratory experiments might not be representative of atmospheric conditions in terms of the RO_2 reaction partner or RO_2 lifetime, warranting further studies on the effects of RO_2 fates on aerosol formation (Boyd et al., 2017; Boyd et al., 2015; Ng et al., 2008; Schwantes et al., 2015).

232 In the condensed phase, organic nitrates can undergo hydrolysis reactions producing HNO_3
233 (Darer et al., 2011; Hu et al., 2011; Rindelaub et al., 2015; Boyd et al., 2015; Szmigielski et al.,
234 2010; Sato, 2008; Jacobs et al., 2014; Bean and Hildebrandt Ruiz, 2016). However, the
235 hydrolysis rate varies greatly with the structure of nitrate (Bean and Hildebrandt Ruiz, 2016;
236 Darer et al., 2011; Hu et al., 2011; Boyd et al., 2015; Rindelaub et al., 2016). Here we assume a
237 first-order irreversible reactive uptake for the heterogeneous loss of organic nitrates onto aerosols
238 (R1), followed by its hydrolysis reaction returning HNO_3 and alcohols (R2) (Fisher et al., 2016):

$$RONO_2(g) \xrightarrow{k_1} AONJ(aq) \tag{R1}$$

$$AONJ(aq) + H_2O \xrightarrow{k_2} ROH + HNO_3(g) \tag{R2}$$

239 where $RONO_2$, AONJ and ROH represent gas- and particle-phase organic nitrates and alcohols
240 respectively. We allow heterogeneous loss of organic nitrates to sulfate, black carbon, primary
241 organic carbon, sea salt, mineral dust and SOA following Mao et al. (2013a). Besides the base
242 case that only includes ISOPNB for heterogeneous loss (Jacobs et al., 2014), we include two
243 additional sensitivity tests to evaluate the potential impact of organic nitrate hydrolysis. One is
244 "hydro_full" case including heterogeneous loss of a C_5 dihydroxy dinitrate (DHDN) and
245 monoterpene nitrates only from OH oxidation during daytime (TERPN1; nighttime monoterpene
246 nitrates are excluded), and the other one is "no_hydro" case assuming no heterogeneous loss for
247 any organic nitrates. We adopt an effective uptake coefficient 0.005 for ISOPNB and DHDN,
248 and 0.01 for TERPN1, following Fisher et al. (2016), with a 3-h bulk lifetime in particle phase
249 (Pye et al., 2015; Lee et al., 2016) (Table S3). Details of each case are listed in Table 2.

250 **3 Observational datasets**

251 We use measurements from a series of field campaigns (2004 ICARTT, 2013 SENEX, and 2013
252 SEAC[4]RS) to evaluate model performance on O_3, NO_x, HNO_3, PAN, $\sum ANs$ and NO_y over the
253 Southeast U.S. in summer.

254 The ICARTT aircraft campaign provided a detailed characterization of tropospheric chemistry
255 over the eastern U.S. in the summer of 2004 (July 1 - August 15, 2004). Two aircrafts, the
256 NASA DC-8 and the NOAA WP-3D, were deployed to collect measurements of ozone, RON,
257 isoprene and its oxidation products. Here we focus on data including O_3, NO_x, HCHO (Tunable
258 Diode Laser (TDL) absorption spectrometry), HNO_3 (mist chamber/IC by University of New
259 Hampshire and Chemical Ionization Mass Spectrometer (CIMS) by California Institute of
260 Technology), PAN and $\sum ANs$ (including gas and aerosol $RONO_2$) collected on the NASA DC-8
261 aircraft over the Southeast U.S. Details of the instrument operation and accuracy are summarized
262 in Singh et al. (2006) and references therein.

263 Two aircraft campaigns were conducted in the summer of 2013 over the Southeast U.S. The first
264 one is NOAA SENEX campaign, using NOAA WP-3D aircraft to investigate the interaction
265 between biogenic and anthropogenic emissions and the formation of secondary pollutants (May

266 27 - July 10, 2013). We focus on daytime measurements of O_3, NO_x, HNO_3, PAN, speciated
267 $RONO_2$ and NO_y in this work. Details of the instrument operation and accuracy are summarized
268 in Warneke et al. (2016) and references therein. The second one is NASA SEAC[4]RS campaign,
269 which took place in August - September of 2013, with a focus on vertical transport of
270 atmospheric pollutants from the surface to the stratosphere. Here we focus on observations of O_3,
271 NO_2, HCHO (laser-induced fluorescence, LIF), $\sum$ANs (including gas and aerosol $RONO_2$) and
272 speciated $RONO_2$ collected on NASA DC-8 aircraft to evaluate model representation of $\sum$ANs
273 and several $RONO_2$ originating from isoprene oxidation. Details of the instrument operation and
274 accuracy are summarized in Toon et al. (2016) and references therein.

275 Besides these aircraft campaigns, we also use surface observations for model evaluation,
276 including nitrate (NO_3^-) wet deposition flux and concentration from the National Trends Network
277 (NTN) of NADP (accessible at http://nadp.sws.uiuc.edu/data/) and surface O_3 and NO_y from
278 EPA AQS (accessible at https://aqs.epa.gov/aqsweb/documents/data_mart_welcome.html). We
279 focus on NO_3^- wet deposition fluxes at 53 NADP sites (Figure 3) and MDA8 O_3 at 157 EPA
280 AQS sites (Figure S2S3) in the Southeast U.S. during July - August of 2004 and 2013. NO_y
281 measurements at 10 out of the 157 AQS sites in the same episodes are compared with model
282 estimates as an additional constraint on the decadal change of NO_y. We choose July – August as
283 our 'summer' since this is the common period of all the measurements used in model evaluation.

4 Model evaluation

285 We evaluate our model against observations from aircraft campaigns in 2004 and 2013. For each
286 of the three field campaigns, all measurements are averaged to a 1-min time resolution. Data
287 from biomass burning ($CH_3CN \geq 225$ ppt or HCN ≥ 500 ppt), urban plumes ($NO_2 \geq 4$ ppb or
288 $NO_x/NO_y \geq 0.4$ (if NO_y is available)), and stratospheric air ($O_3/CO > 1.25$ mol mol^{-1}) are
289 excluded (Hudman et al., 2007) in all the analyses, as these subgrid processes may not be well
290 represented in our model. We focus on the Southeast U.S. region, using data within the domain
291 of 25 - 40° N latitude and 100 - 75° W longitude for our analyses. A map of all the flight tracks
292 of each campaign is shown in Figure S3S4. All model results are sampled along the flight track
293 with 1-min time resolution.

4.1 Mean vertical profiles of O_3 and RON

295 Figure 1 shows the observed and modeled mean vertical profiles of O_3, NO_x, HNO_3, PAN,
296 $\sum$ANs and NO_y during ICARTT and SENEX. We use $\sum$ANs measurements from SEAC[4]RS to
297 evaluate model performance during summer 2013, due to the lack of $\sum$ANs measurements from
298 SENEX. Our model results include both gas and aerosol $RONO_2$ in $\sum$ANs, although aerosol
299 $RONO_2$ accounts for 7~11% of $\sum$ANs in the planetary boundary layer (PBL, < 1.5 km). We do
300 not consider inorganic nitrates in particle phase in this analysis, due to lack of thermodynamic
301 model for inorganic aerosols in current version of AM3. This simplification is expected to have

minimal effects, as they only account for a small fraction of aerosol nitrates in the Southeast U.S. (Ng et al., 2017). To investigate the impact of $RONO_2$ hydrolysis, we include two model simulations, the base case with heterogeneous loss of ISOPNB, and a sensitivity run 'no_hydro' without heterogeneous loss of organic nitrates.

Mean observed O_3 in the surface layer decreased from 50 ppb during ICARTT to 35 ppb during SENEX, consistent with the declining trend in surface MDA8 ozone at AQS monitoring sites (section 5.2). As we show in section 5.2, this decline in ozone is mainly driven by NO_x emission reduction, with little influence by meteorology in the two years. Our model can reproduce the vertical gradient and the relative change of O_3 from 2004 to 2013, except for a positive absolute bias of 6 - 12 ppb in the boundary layer. Performance statistics of O_3 in the boundary layer listed in Table S4 also indicate positive biases in the model, with the fractional bias (FB) of 9.4 – 17%, fractional error (FE) of 16 – 19 %, normalized mean bias (NMB) of 9.4 – 16% and normalized mean error (NME) of 16 – 19 %. This overestimate of O_3 is higher than that reported (3 - 5 ppb) by Mao et al. (2013b) for their simulation of the ICARTT dataset, likely due to faster photolysis of carbonyl nitrates that increases the NO_x recycling efficiency from isoprene oxidation.

We further examine mean vertical profiles of NO_x and its reservoirs in 2004 and 2013 (Figure 1). In the boundary layer along the flight tracks, HNO_3 is the most abundant RON, accounting for 40 - 46 % of NO_y, followed by NO_x (18 - 23 %), PAN (20 %), and $\sum$ANs (11 - 21 %). Between 2004 and 2013, mean observed NO_y in the boundary layer decreased by 20 %, from 2.0 ppb to 1.6 ppb, a weaker change than the 35 % reduction of total NO_x emissions (Table 1). The responses of major RON are mostly proportional to the change in NO_x emissions, with the notable exception of $\sum$ANs. We find significant decreases in NO_x (- 35 %) and HNO_3 (- 29 %) as well as a slight decrease in PAN (- 13 %) from observations. The relative trends of HNO_3 and PAN are opposite to those found in the Los Angeles (LA) basin, where PAN decreased much faster than HNO_3 (Pollack et al., 2013). This difference results mainly from the rapid decrease of anthropogenic VOC emissions in the LA basin that also serves as major precursors of PAN. In contrast, isoprene is the major precursor of PAN over the Southeast U.S. Its emissions show a constant supply (within 5 % differences over the two summers) in this region. $\sum$ANs shows a different trend from the above compounds, increasing from 0.23 ppb to 0.27 ppb (+ 17 %) near the surface. As we show below in section 5.1, these changes (except for $\sum$ANs) are mostly consistent with model estimates on a regional average. Discrepancy in their trends of vertical profiles and regional average might be due to representative errors from the three aircraft campaigns on spatial (Figure S3S4) and temporal (different episodes, referring to observation data description in section 3) scales.

The model can well reproduce RON in the boundary layer but tend to underestimate them in the free troposphere. This is likely due to insufficient production of NO_x from lightning in the free troposphere in our model, which is 0.048 Tg N in total over North America during July - August of 2004, lower by almost a factor of 5 compared to the value (0.27 Tg N from July 1-August 15,

340 2004) reported by Hudman et al. (2007). This underestimate can be improved by scaling up
341 lightning emission by a factor of 5-10 (Fang et al., 2010). We do not adjust the lightning NO_x
342 emissions in this work due to its high uncertainty (Ott et al., 2010; Pickering et al., 1998).

343 Hydrolysis of organic nitrates affects $RONO_2$ significantly in the boundary layer. By introducing
344 hydrolysis of ISOPNB, we find that model relative bias of ∑ANs is reduced from + 20 % to + 2 %
345 during ICARTT (Figure 1). Performance metrics in Table S4 also indicate better agreement of
346 the model with observations if hydrolysis of ISOPNB assumed. However, the relative bias is
347 increased in magnitude from – 9 % to – 24 % during SEAC^{4}RS. This low bias can be partially
348 due to neglecting small alkyl nitrates, which could contribute 20 - 30 ppt to ∑ANs (less than 10%
349 near the surface) during SEAC^{4}RS (Fisher et al., 2016). Including small alkyl nitrates will
350 increase modeled ∑ANs a bit in ICARTT as well. Hydrolysis of ISOPNB also leads to a slight
351 increase of HNO_3 (Table S4). The impact of hydrolysis of ISOPNB on boundary layer O_3
352 appears to be small. This is mainly because without hydrolysis, the dominant loss of ISOPNB is
353 oxidation by OH, which then leads to the formation of secondary organic nitrates including
354 MVKN, MACRN and DHDN. The majority of these organic nitrates (MVKN and DHDN)
355 return NO_x slowly due to their long lifetimes (Table S5), resulting in a similar effect on ozone
356 production as hydrolysis of ISOPNB. In addition to the good agreement of ∑ANs, our model
357 shows good agreement with speciated $RONO_2$ measured during SENEX and SEAC^{4}RS,
358 including ISOPN and the sum of MVKN and MACRN (Figure 2). We find that the large
359 discrepancy between ∑ANs and speciated alkyl nitrates (Figure S4S5) can be explained by a
360 combination of monoterpene nitrates and DHDN and nighttime NO_3 oxidation products from
361 isoprene, accounting for 20 - 24 %, 14 - 17 % and 23 - 29 % of ∑ANs respectively in the
362 boundary layer.

363 Given the good agreement between observed and modeled RON in both 2004 and 2013, we find
364 that the ozone bias, shown in Figure 1, cannot be completely explained by an overestimate of
365 anthropogenic NO_x emissions. A recent GEOS-Chem study (Travis et al., 2016) shows that the
366 ozone bias in their model can be largely reduced by scaling down anthropogenic NO_x emissions.
367 We find that a similar reduction of anthropogenic NO_x emissions in 2013, from 0.25 Tg N mon^{-1}
368 to 0.15 Tg N mon^{-1}, would lead to an underestimate of NO_y, HNO_3 and PAN by 30 %, 33 % and
369 30 %, respectively. Such a reduction would be also inconsistent with the relative changes in EPA
370 estimates of NO_x emissions shown above. Indeed, other processes, such as ozone dry deposition,
371 may also contribute to this bias and warrant further investigation.

4.2 NO_3^- wet deposition flux and concentration

373 Figure 3 shows a comparison of NO_3^- wet deposition flux between observations and model
374 results during the summers of 2004 and 2013. The observed NO_3^- wet deposition flux is
375 calculated by multiplying the measured NO_3^- concentration and precipitation at each monitoring

376 site as $F_{o,i}=C_{o,i}P_{o,i}$, where $F_{o,i}$ is the monthly-mean NO_3^- wet deposition flux, $C_{o,i}$ and $P_{o,i}$ are the

377 monthly-mean observed NO_3^- concentration precipitation at monitoring site i. The modeled NO_3^-

378 wet deposition flux includes HNO_3 and all the alkyl nitrates. Observations indicate a 24 %

379 reduction of NO_3^- wet deposition flux in summer from 2004 to 2013 over the Southeast U.S.,

380 likely due to NO_x emission reductions. This reduction in monthly averaged NO_3^- wet deposition

381 flux is well captured by our model (-29 %), despite a low relative bias of 40 % in both years and

382 NMB of - 39 – - 43 % (Table S4).

383 Since errors in modeled precipitation could strongly affect the modeled NO_3^- wet deposition flux

384 (Appel et al., 2011; Grimm and Lynch, 2005; Metcalfe et al., 2005; Paulot et al., 2014; Tost et al.,

385 2007), we also evaluate the modeled NO_3^- concentration ($C_{p,i}$), which is calculated by using the

386 modeled NO_3^- wet deposition flux ($F_{p,i}$) and observed precipitation ($P_{o,i}$; $C_{p,i}=F_{p,i}/P_{o,i}$), as a

387 separate constraint. The model shows a similar declining trend from the observations with a

388 relative bias of - 23 % and – 41 % on NO_3^- concentration for 2004 and 2013 respectively. Our

389 results are consistent with the base case of Paulot et al. (2016), which showed that convective

390 removal is likely insufficient in AM3, leading to underestimates of both NO_3^- wet deposition flux

391 and concentrations. Our results are somewhat different from a recent GEOS-Chem study (Travis

392 et al., 2016). They found that reducing anthropogenic NO_x emissions from NEI11v1 by 53 % can

393 significantly improve the overestimate of 71 % on NO_3^- wet deposition flux in their model during

394 August-September of 2013. A further reduction of anthropogenic NO_x emissions in our model

395 (to 0.15 Tg N mon^{-1}), as suggested by Travis et al. (2016), would lead to an even greater negative

396 bias compared to observations.

397 **4.3 $RONO_2$ and related species**

398 We further evaluate $RONO_2$ and related species in this section, with a large focus on

399 measurements from ICARTT and SEAC[4]RS. The major pathway for the production of daytime

400 $RONO_2$ is the reaction of NO with RO_2 originating from VOC oxidation by OH:

$$RH + OH + O_2 \rightarrow RO_2 + H_2O \qquad (R3)$$

$$NO + RO_2 \rightarrow (1 - \alpha) NO_2 + \alpha\, RONO_2 + HCHO + products \qquad (R4)$$

401 where α is the branching ratio for alkyl nitrate formation. NO_2 subsequently undergoes

402 photolysis to produce O_3:

$$NO_2 + h\nu \xrightarrow{O_2} O_3 + NO \qquad (R5)$$

403 For isoprene, α is 9 ± 4 % (for ISOPN) according to a recent study (Xiong et al., 2015). For
404 monoterpenes, specifically α-pinene, α ranges from 1 % to 26 % (Rindelaub et al., 2015;
405 Nozière et al., 1999; Aschmann et al., 2002). Here, we use 10 % for isoprene and 26 % for
406 monoterpenes. As $RONO_2$ and O_3 are both produced from (R4), a correlation between them is
407 expected. We show that the model can roughly reproduce the correlation of O_x (= O_3 + NO_2) vs.
408 $\sum$ANs during both ICARTT and SEAC^{4}RS (Figure 4), although the slope has a positive relative
409 bias of about 21 % and 33 % respectively, largely due to an overestimate of O_3 in the model. The
410 good agreement between observed and modeled O_x vs. daytime $RONO_2$ provides additional
411 support for our treatment of the yields and fate of these daytime isoprene nitrates.

412 Another metric to evaluate $RONO_2$ chemistry is the correlation between $\sum$ANs and HCHO, as
413 the latter is a coproduct from (R4). We show in Figure 4 that the model can roughly capture the
414 observed $\sum$ANs-HCHO slope, with an underestimate by 25 % and 13 % during ICARTT and
415 SEAC^{4}RS, respectively. The underestimate is in part due to small alkyl nitrates that are neglected
416 in the model, as mentioned in section 4.1. During ICARTT, the slope estimated by AM3 is 0.12,
417 similar to the value (0.15) from a previous GEOS-Chem study using a different isoprene
418 oxidation mechanism that assumed a higher α (of 4.7% from ISOPNB and 7.0% from ISOPND
419 vs. 10 % of ISOPNB and zero ISOPND in AM3) and a lower yield of HCHO (66 % vs. 90 % in
420 AM3) (Mao et al., 2013b). The reason for such similarity between the two models might be two-
421 fold: (a) the additional contribution of monoterpene nitrates to $\sum$ANs in AM3 compensates for
422 the decrease in α from isoprene nitrates compared to GEOS-Chem and (b) the coarse grid
423 resolution of GEOS-Chem simulation (2° x 2.5°) may lead to a higher estimate of HCHO
424 compared to the result from a finer grid resolution (Yu et al., 2016).

425 Since HCHO can be produced from other pathways of isoprene hydroxyl peroxy radicals
426 (ISOPO$_2$) besides (R4) (such as isomerization of ISOPO$_2$ and ISOPO$_2$ + HO$_2$), changes in the
427 slope of $\sum$ANs vs. HCHO may help to quantify decadal changes in isoprene oxidation pathways.
428 We find in Figure 4 that the observed slope of $\sum$ANs-HCHO shows very little change from 2004
429 to 2013. This is in part due to substantial HCHO production from isoprene oxidation under low
430 NO$_x$ conditions (Li et al., 2016), and in part due to the buffering of $\sum$ANs in response to
431 decreasing NO$_x$, as shown below in section 5.1. Our model is able to reproduce such behavior.
432 We also find that the branching ratios for the reactions of ISOPO$_2$ change marginally from 2004
433 to 2013 over the Southeast U.S. (Figure S5S6). The fraction of ISOPO$_2$ + NO has decreased from
434 81 % in 2004 to 66 % in 2013. The fraction of ISOPO$_2$ + HO$_2$ has increased from 15 % to 28 %,
435 and the fraction of ISOPO$_2$ isomerization has increased from 4 % to 6 %. Our result is slightly
436 different from the results of GEOS-Chem, which found a lower contribution from the NO
437 pathway (54 %) and higher from isomerization (15 %) during August - September of 2013
438 (Travis et al., 2016).

439 We also compare the correlation between major daytime isoprene nitrates and HCHO during
440 2013, which provides a constraint on the yield of these nitrates. Our model shows a slight

441 overestimate on the slope (Figure 4 (b)), consistent with comparison of mean vertical profiles
442 shown in Figure 2. The computed slope (5 %) in this study is different from that (2.5 %) of a
443 recent GEOS-Chem simulation by Fisher et al. (2016). This is partially due to the different
444 treatment of β- and δ-ISOPO$_2$ between GEOS-Chem and AM3. Another factor is that MVKN
445 and MACRN are not allowed to hydrolyze in AM3, leading to higher abundance of these two
446 nitrates.

447 Figure 5 shows the mean vertical profiles of modeled monoterpene nitrates (MNs) and isoprene
448 nitrates (INs) during ICARTT and SEAC^{4}RS. INs are the most abundant RONO$_2$, accounting for
449 76-80 % below 3 km over the Southeast U.S. In the measurements, ISOPN + MVKN + MACRN
450 only contribute one third of the total INs (Figure S4S5). We show below that the discrepancy of
451 $\sum$ANs and speciated RONO$_2$ can be explained by other daytime and nighttime INs as well as
452 MNs in the model. More than 60 % of modeled INs originate from isoprene oxidation during
453 daytime. The first-generation nitrate ISOPN contributes slightly more (31 %) than the second-
454 generation nitrates MVKN + MACRN (28 %) to the total daytime INs during ICARTT. This is
455 different from Mao et al. (2013b) who showed a higher contribution of MVKN + MACRN than
456 the first-generation INs, due to the different treatment of β- and δ-ISOPO$_2$. We see more ISOPN
457 (32 %) than MVKN + MACRN (26 %) from the daytime INs during SEAC^{4}RS, consistent with
458 Fisher et al. (2016). A large uncertainty in our model is attributed to DHDN, which contributes
459 32 % to the daytime INs. Fisher et al. (2016) showed less DHDN during SEAC^{4}RS since it was
460 removed rapidly by hydrolysis (1-h lifetime) in their model. Our sensitivity test (hydro_full,
461 Figure S6S2) indicates that AM3 would significantly underestimate $\sum$ANs if we assume a
462 similar heterogeneous loss of DHDN as ISOPN. In fact, DHDN was hypothesized originally in
463 Lee et al. (2014) for the imbalance of nitrogen in their lab experiments, and may serve as a proxy
464 for a large number of unidentified daytime INs. It remains unclear what the dominant loss of
465 DHDN is. Daytime nitrates from monoterpene oxidation are another important source of $\sum$ANs
466 in this region, accounting for 17 - 20 % (24 - 26 ppt) of the total. Fisher et al. (2016) estimate a
467 smaller burden of MNs, of about 10 - 20 ppt due to a lower molar yield (18 % vs. 26 % in AM3)
468 and faster hydrolysis of MNs in their model.

469 Nighttime chemistry contributes about 30 - 36 % of $\sum$ANs, which is dominated by isoprene
470 oxidation as well (Figure 5). 33 - 41 % of the INs are produced during night, similar to the value
471 (44 %) reported by Mao et al. (2013b) but with different speciation, due to the different treatment
472 of chemistry. PROPNN contributes about 29-38 % of the total INs. PROPNN in this work is
473 mainly produced from the oxidation of C5 nitrooxy hydroperoxide (INPN) and C5 carbonyl
474 nitrate (ISN1; dominantly by photolysis) that are generated from isoprene oxidation by NO$_3$
475 during the nighttime. This is different from Fisher et al. (2016), who showed that PROPNN is
476 partially from the δ-ISOPO$_2$ + NO pathway and partially from the oxidation of ISN1 by NO$_3$. In
477 our model, we see a rapid increase of PROPNN after sunrise in the boundary layer (Figure S7),
478 consistent with observations at the Southern Oxidants and Aerosols Study (SOAS) ground site
479 CTL (Schwantes et al., 2015). Our model overestimates the mean vertical profile of PROPNN by

480   a factor of 3 (not shown). As our model may largely underrepresent the chemical complexity of
481   nighttime isoprene oxidation as shown by Schwantes et al. (2015), we consider PROPNN as a
482   proxy for other unspecified isoprene nighttime nitrates. Over all, PROPNN contributes a
483   significant fraction of $\sum$ANs in the model, 23 - 29 % in the boundary layer as shown in section
484   4.1. With monoterpene nitrates and isoprene derived DHDN and nighttime NO_3 oxidation
485   products taken into account, we find that model can well reproduce both observed $\sum$ANs and
486   speciated alkyl nitrates (Figure S4S5).

5 Decadal Change of PBL RON and surface ozone over SEUS

488   As RON and related species from aircraft and surface measurements are well reproduced in our
489   model for both 2004 and 2013, we assume that the model is representative of this chemical
490   environment, and then use the model to derive monthly mean changes between 2004 and 2013.
491   We also investigate the impacts of further decreases in NO_x emissions by applying a hypothetical
492   40 % reduction of anthropogenic NO_x emissions of 2013 but keeping other emissions and
493   meteorology the same ("hypo" case in Table 2).

5.1 RON

495   We first examine the simulated decadal change of RON in the boundary layer over the Southeast
496   U.S. as shown in Figure 6. In summer of 2004, the model suggests that NO_y is mainly comprised
497   of HNO_3 (45 %), NO_x (31 %), $\sum$PNs (14 %) and $\sum$ANs (9 %). In response to a 40 % reduction in
498   anthropogenic NO_x emissions (35 % reduction in total NO_x emissions, Table 1) from 2004 to
499   2013, NO_y declined by 34 %. This modeled response is comparable to long-term NO_y
500   measurements from the AQS surface network, which shows on average a 45 % decrease from
501   2004 to 2013 over the Southeast U.S. Based on model estimates in Figure 6, most RON are
502   reduced proportionally, with decreases of 38 % for HNO_3, 32 % for NO_x and 34% for $\sum$PNs. The
503   different change in $\sum$PNs and PAN (the majority of $\sum$PNs) in Figure 1 might be due to the
504   difference in sampling regions. The only exception is $\sum$ANs, with a smaller decline of 19 %. As
505   an important source of organic aerosols (OA), $\sum$ANs may contribute to the decrease of OA over
506   the Southeast U.S. in the past decade (Blanchard et al., 2016).

507   We conducted a sensitivity test with an additional 40 % reduction of anthropogenic NO_x
508   emissions from 2013. We find that NO_y decreases by 29 %, with a proportional decrease in
509   HNO_3, NO_x, and $\sum$PNs (Figure 6). The slower decrease of NO_y is likely due to $\sum$ANs, which
510   decrease at a slower rate and becomes a larger fraction of NO_y. The buffering of $\sum$ANs is
511   consistent with previous studies (Browne and Cohen, 2012; Fisher et al., 2016), mainly due to
512   lower OH resulting from decreased NO_x (Figure S8) and thus a prolonged lifetimes of NO_x and
513    $\sum$ANs (Browne and Cohen, 2012). As shown in Figure S8, averaged noontime OH decreases by
514   11 % from 2004 to 2013 and by 29 % after we impose an additional 40 % NO_x emission
515   reduction from 2013 levels.

516 The historical NO$_x$ emission reduction also affects reactive nitrogen export out of the boundary
517 layer. Here we define exported nitrogen as the difference of the sources (chemical production
518 and emissions) and sinks (chemical loss, wet and dry deposition). As shown in Table 3, total
519 summertime NO$_y$ export from the Southeast U.S. boundary layer decreases proportionally, from
520 24.1 Gg N in 2004 to 16.6 Gg N in 2013. The NO$_y$ export efficiency, calculated as net exported
521 nitrogen divided by total NO$_x$ emissions, remains roughly the same (12 %) for 2004 and 2013,
522 comparable to previous studies (Fang et al., 2010; Li et al., 2004; Parrish et al., 2004; Mao et al.,
523 2013b; Sanderson et al., 2008; Hudman et al., 2007). Among all exported species,
524 NO$_x$ contributes most of net export from the PBL (6 % of total NO$_x$ emissions), followed by
525 PAN (4 %) and $\sum$ANs (2 %). We emphasize in Table 3 that a major fraction of NO$_x$ is exported
526 through the top of the boundary layer (convection). From a budget calculation throughout the
527 tropospheric column over the same region, we find that despite being the same NO$_y$ export
528 efficiency (12 %), HNO$_3$ becomes the major exporter, accounting for half of NO$_y$ export
529 efficiency from the total column (6 %). The contributions from PAN and $\sum$ANs are roughly the
530 same as their export from the boundary layer (4 % and 2 %). This suggests that surface
531 NO$_x$ ventilated through the boundary layer, converted to HNO$_3$ in the free troposphere and
532 exported as HNO$_3$ is likely the major NO$_y$ export mechanism over the Southeast U.S. in our
533 model, which is in agreement with previous observations (Parrish et al., 2004; Neuman et al.,
534 2006). PAN and $\sum$ANs together account for another half of NO$_y$ export efficiency. As PAN
535 and $\sum$ANs are of biogenic origin and longer lived than HNO$_3$, they may play a key role in
536 influencing RON and ozone in downwind regions (Moxim et al., 1996; Fischer et al., 2014).

537 **5.2 Surface ozone**

538 Since the mid-1990s, NO$_x$ emission controls have led to significant improvement on ozone air
539 quality over the eastern U.S. (Simon et al., 2015; Cooper et al., 2012). As NO$_x$ emissions
540 continue to decrease, ozone production efficiency (OPE) may increase due to the lower NO$_x$
541 removal rate by OH and to some extent may compensate the ozone reduction (Sillman, 2000).
542 Meanwhile, surface ozone production may be further complicated by the increasing importance
543 of RO$_2$ isomerization and RO$_2$ + HO$_2$. Here we first evaluate our model against surface ozone
544 observations in 2004 and 2013, and then project the future response of surface ozone to even
545 lower NO$_x$ emissions to examine the efficacy of near-term NO$_x$ emission controls at lowering
546 near-surface ozone levels.

547 We first examine the modeled surface ozone against observations at 157 EPA AQS monitoring
548 sites over the Southeast U.S. in July-August of 2004 and 2013 (Figure S9). In general, AM3
549 overestimates surface MDA8 ozone in both years by about 16 ppb on average, with the NMB of
550 33 - 45 % and NME of 35 - 46 % respectively. This positive bias of summertime surface O$_3$ has
551 been a common issue to a number of modeling studies of this region (Fiore et al., 2009; Canty et
552 al., 2015; Brown-Steiner et al., 2015; Strode et al., 2015; Travis et al., 2016). This might be
553 partially attributed to overestimated anthropogenic NO$_x$ emissions from non-power plant sectors,

554 excessive vertical mixing in the boundary layer (Travis et al., 2016) or underestimates of O_3 dry
555 deposition (Hardacre et al., 2015; Val Martin et al., 2014). Further studies are warranted to
556 investigate the cause of this bias in AM3.

557 Surface O_3 concentrations over the Southeast U.S. decline substantially from 2004 to 2013 in
558 response to the large NO_x emission reduction (Simon et al., 2015). MDA8 ozone averaged across
559 all the monitoring sites is observed to decrease by 11 ppb (23 % of observed mean MDA8 ozone
560 in July-August of 2004) resulting from approximately 40 % reductions of anthropogenic NO_x
561 emissions (35 % reduction in total NO_x emissions). This strong sensitivity of surface ozone to
562 NO_x emission reflects the linear relationship between ozone production rate and NO_x
563 concentrations when NO_x is low (Trainer et al., 2000). Our model is able to capture this strong
564 NO_x - O_3 sensitivity, with the mean MDA8 ozone reduced by 10 ppb from 2004 to 2013. We
565 find that a further 40 % reduction of anthropogenic NO_x emissions with identical meteorological
566 conditions could lead to an additional 9 ppb decrease, a similar magnitude to the change from
567 2004 to 2013.

568 We further investigate the impact of temperature and moisture on surface O_3 from 2004 to 2013.
569 While several studies suggest that surface O_3 increases with ambient temperature (Jacob and
570 Winner, 2009; Bloomer et al., 2010; Wu et al., 2008; Steiner et al., 2010), Cooper et al. (2012)
571 showed that this temperature related impact is weak during the period of 1990-2010 across the
572 U.S.A. Recent studies suggest that relative humidity (RH) or vapor pressure deficit (VPD) may
573 play an important role in ozone variability through soil-atmosphere or biosphere-atmosphere
574 coupling (Kavassalis and Murphy, 2017; Camalier et al., 2007; Tawfik and Steiner, 2013). Our
575 model shows marginal differences in RH (less than 1 %) and temperature (+ 2.4 K) within the
576 PBL over the Southeast U.S. between the summers of 2004 and 2013, consistent with observed
577 changes of RH (+ 2.7 %) and temperature (+ 2.6 K) during ICARTT and SENEX. This small
578 variation in the model is also consistent with climatology data (Hidy et al., 2014). Camalier et al.
579 (2007) showed that RH has a much bigger impact on summertime ozone than temperature over
580 the Southeast U.S., suggesting little influence of meteorology on ozone trend. Using the same
581 model but with the standard AM3 chemical mechanism, Lin et al. (2017) found that meteorology
582 changes would have caused high surface ozone over the eastern U.S. to increase by 0.2 - 0.4 ppb
583 yr^{-1} in the absence of emission controls from 1988 to 2014. Therefore, we conclude that the
584 impact of climate variability and change on O_3 is relatively small compared to NO_x emission
585 reductions over the Southeast U.S., consistent with previous studies (Lam et al., 2011; Hidy et al.,
586 2014; Lin et al., 2017; Rieder et al., 2015).

587 Decreasing NO_x emissions also reduces the frequency of high O_3 pollution events. Figure 7
588 shows the probability density function of observed and modeled MDA8 ozone at each
589 monitoring site during July-August of 2004 and 2013, and the probability density function of
590 modeled MDA8 ozone under a hypothetical scenario with another 40 % reduction in
591 anthropogenic NO_x emissions compared to 2013. We show that the lowest O_3, about 20 ppb in
592 current model simulations, remains invariant with NO_x emission changes over the Southeast U.S.,

consistent with observations (Figure 7 (a)). Meanwhile, the high tail of MDA8 ozone events has shifted from more than 100 ppb in 2004 to about 85 ppb after the 40 % reduction of anthropogenic NO_x emissions from 2013. A similar shift is found in observations. The narrowing of the range of O_3 with decreasing NO_x is consistent with the observed trends reported by Simon et al. (2015). We also find that further reductions of NO_x emissions will reduce both median O_3 values and the high tail, suggesting that fewer high ozone events will occur under continued NO_x emission controls in the future.

6 Conclusions and Discussions

Near-surface ozone production over the Southeast U.S. is heavily influenced by both anthropogenic and biogenic emissions. We investigate the response of NO_y speciation to the significant NO_x emission controls (about 40 % reduction) in this region over the past decade, in light of the fast-evolving understanding of isoprene photooxidation. This knowledge is needed to predict nitrogen and ozone budgets in this region and elsewhere in the world with similar photochemical environments. Here we use extensive aircraft and ground observations, combined with a global chemistry-climate model (GFDL AM3), to examine decadal changes in NO_y abundance and speciation as well as in surface O_3 mixing ratios over the Southeast U.S. between the summers of 2004 and 2013. We then use the model to infer future NO_y speciation and surface ozone abundances in response to further NO_x emission controls in this region.

We first evaluate the model with aircraft and surface observations. When we apply the estimated 40 % reductions in anthropogenic NO_x emissions from 2004 to 2013, our model reproduces the major features of vertical profiles of NO_x, HNO_3, PAN, $\sum$ANs and NO_y observed during aircraft campaigns over the Southeast U.S. in the summers of 2004 and 2013. By including recent updates to isoprene oxidation, our model can largely reproduce the vertical profiles of $\sum$ANs and several speciated alkyl nitrates, as well as their correlations with O_x and HCHO, lending support to the model representation of isoprene oxidation. On the other hand, we show that a discrepancy between measured $\sum$ANs and speciated $RONO_2$ can be explained by a combination of monoterpene nitrates, dinitrates and nighttime NO_3 oxidation products from isoprene. We also show that modeled ozone appears to be insensitive to hydrolysis of ISOPNB, because its photooxidation, mainly by OH, also returns little NO_x.

Major RON decline proportionally as a result of NO_x emission reductions in the Southeast U.S., except for a slower rate in $\sum$ANs. The slower decline of $\sum$ANs reflects the prolonged lifetime of NO_x when it is decreasing. Our model suggests that summertime monthly averaged NO_x, HNO_3, PAN, and NO_y decline by 30 - 40 %, in response to 40 % reduction in anthropogenic NO_x emissions from 2004 to 2013. This proportional decrease is likely driven by high concentrations of biogenic VOCs, the major precursor of PAN in this region that change little in magnitude from 2004 to 2013. In contrast, Pollack et al. (2013) find a faster PAN decrease than HNO_3 in the LA basin over the past several decades, partly due to the decrease in anthropogenic VOC emissions that are major PAN precursors.

631   Deposited and exported NO_y decline with NO_x emission reductions. The model also shows a

632   decrease of NO_3^- wet deposition flux by 29 % from 2004 to 2013, consistent with observations

633   from the NADP network (- 24 %). We find from model calculations that the NO_y export

634   efficiency remains at 12 % in both 2004 and 2013, leading to a proportional decrease of exported

635   NO_y. The dominant NO_y export terms include NO_x or HNO_3, each accounting for 6% of the total

636   exported NO_y, followed by $\sum PNs$ (4 %) and $\sum ANs$ (2 %).

637   The response of surface ozone to NO_x emission reductions reveals a strong $NO_x - O_3$ sensitivity

638   in summertime over the Southeast U.S. Observations from EPA AQS surface network suggest

639   that mean MDA8 ozone during July-August has decreased by 23%, from 48 ppb in 2004 to 37

640   ppb in 2013. Despite a positive absolute bias of up to 12 ppb in boundary layer ozone and 16 ppb

641   in surface MDA8 ozone, our model shows a 10 ppb decrease of surface MDA8 ozone from 2004

642   to 2013, very close to the observed 11 ppb decrease from the EPA data. The bias of ozone in our

643   model is not entirely attributed to uncertainties in NO_x emissions, as the overestimate suggested

644   by earlier work would lead to an underestimate of NO_y (Travis et al., 2016). Care should be

645   exercised in applying the modeling results for surface ozone regulation purposes, given the high

646   ozone bias shown in our model. We find from model calculations that modeled MDA8 O_3 will

647   continue to decrease by another 9 ppb assuming anthropogenic NO_x emissions are reduced by

648   40 % from 2013 levels with meteorology and other emissions kept the same. In addition, further

649   NO_x emission reduction leads to less frequent high ozone events. This continued strong

650   sensitivity of surface O_3 to NO_x emissions can guide the development of effective emission

651   control strategies for improving future air quality.

652 **Data availability**

653   Observational datasets and modeling results are available upon request to the corresponding

654   author (jmao2@alaska.edu).

655 **Competing interests**

656   The authors declare that they have no conflict of interest.

657 **Acknowledgements**

658   The authors thank Vaishali Naik (NOAA GFDL) for providing emission inventories in the

659   GFDL AM3 model, and Leo Donner (NOAA GFDL) and William Cooke (UCAR/NOAA) for

660   the help with convection scheme of AM3. J.L., J.M. and L.W.H. acknowledge support from the

661   NOAA Climate Program Office grant # NA13OAR431007. J.M., L.W.H. and A.M.F.

662   acknowledge support from NOAA Climate Program Office grant #NA14OAR4310133. J.D.C.

663   and P.O.W. acknowledge support from NASA grants (NNX12AC06G and NNX14AP46G). J.L

664   acknowledge support from the Startup Foundation for Introducing Talent of NUIST grant

665   #2243141701014 and the Priority Academic Program Development of Jiangsu Higher Education

666   Institutions   (PAPD).

References

Anderson, D. C., Loughner, C. P., Diskin, G., Weinheimer, A., Canty, T. P., Salawitch, R. J., Worden, H. M., Fried, A., Mikoviny, T., Wisthaler, A., and Dickerson, R. R.: Measured and modeled CO and NOy in DISCOVER-AQ: An evaluation of emissions and chemistry over the eastern US, Atmos. Environ., 96, 78-87, 2014.

Appel, K., Foley, K., Bash, J., Pinder, R., Dennis, R., Allen, D., and Pickering, K.: A multi-resolution assessment of the Community Multiscale Air Quality (CMAQ) model v4. 7 wet deposition estimates for 2002–2006, Geosci. Model. Dev., 4, 2, 357-371, 2011.

Aschmann, S. M., Atkinson, R., and Arey, J.: Products of reaction of OH radicals with α - pinene, J. Geophys. Res., 107, D14, 2002.

Astitha, M., Luo, H., Rao, S. T., Hogrefe, C., Mathur, R., and Kumar, N.: Dynamic evaluation of two decades of WRF-CMAQ ozone simulations over the contiguous United States, Atmos. Environ., 164, Supplement C, 102-116, 2017.

Ayres, B. R., Allen, H. M., Draper, D. C., Brown, S. S., Wild, R. J., Jimenez, J. L., Day, D. A., Campuzano-Jost, P., Hu, W., de Gouw, J., Koss, A., Cohen, R. C., Duffey, K. C., Romer, P., Baumann, K., Edgerton, E., Takahama, S., Thornton, J. A., Lee, B. H., Lopez-Hilfiker, F. D., Mohr, C., Wennberg, P. O., Nguyen, T. B., Teng, A., Goldstein, A. H., Olson, K., and Fry, J. L.: Organic nitrate aerosol formation via NO_3 + biogenic volatile organic compounds in the southeastern United States, Atmos. Chem. Phys., 15, 23, 13377-13392, 2015.

Baker, K. R., and Woody, M. C.: Assessing Model Characterization of Single Source Secondary Pollutant Impacts Using 2013 SENEX Field Study Measurements, Environ. Sci. Technol., 51, 7, 3833-3842, 2017.

Bates, K. H., Crounse, J. D., St. Clair, J. M., Bennett, N. B., Nguyen, T. B., Seinfeld, J. H., Stoltz, B. M., and Wennberg, P. O.: Gas Phase Production and Loss of Isoprene Epoxydiols, J. Phys. Chem. A, 118, 7, 1237-1246, 2014.

Bates, K. H., Nguyen, T. B., Teng, A. P., Crounse, J. D., Kjaergaard, H. G., Stoltz, B. M., Seinfeld, J. H., and Wennberg, P. O.: Production and Fate of C4 Dihydroxycarbonyl Compounds from Isoprene Oxidation, J. Phys. Chem. A, 120, 1, 106-117, 2016.

Bean, J. K., and Hildebrandt Ruiz, L.: Gas–particle partitioning and hydrolysis of organic nitrates formed from the oxidation of α-pinene in environmental chamber experiments, Atmos. Chem. Phys., 16, 4, 2175-2184, 2016.

Blanchard, C. L., Hidy, G. M., Shaw, S., Baumann, K., and Edgerton, E. S.: Effects of emission reductions on organic aerosol in the southeastern United States, Atmos. Chem. Phys., 16, 1, 215-238, 2016.

Bloomer, B. J., Vinnikov, K. Y., and Dickerson, R. R.: Changes in seasonal and diurnal cycles of ozone and temperature in the eastern U.S, Atmos. Environ., 44, 21–22, 2543-2551, 2010.

703 Boyd, C. M., Sanchez, J., Xu, L., Eugene, A. J., Nah, T., Tuet, W. Y., Guzman, M. I., and Ng, N.
704 L.: Secondary organic aerosol formation from the β-pinene+NO3 system: effect of humidity and
705 peroxy radical fate, Atmos. Chem. Phys., 15, 13, 7497-7522, 2015.

706 Boyd, C. M., Nah, T., Xu, L., Berkemeier, T., and Ng, N. L.: Secondary Organic Aerosol (SOA)
707 from Nitrate Radical Oxidation of Monoterpenes: Effects of Temperature, Dilution, and
708 Humidity on Aerosol Formation, Mixing, and Evaporation, Environ. Sci. Technol., 51, 14, 7831-
709 7841, 2017.

710 Brown-Steiner, B., Hess, P. G., and Lin, M. Y.: On the capabilities and limitations of GCCM
711 simulations of summertime regional air quality: A diagnostic analysis of ozone and temperature
712 simulations in the US using CESM CAM-Chem, Atmos. Environ., 101, 134-148, 2015.

713 Browne, E. C., and Cohen, R. C.: Effects of biogenic nitrate chemistry on the NOx lifetime in
714 remote continental regions, Atmos. Chem. Phys., 12, 24, 11917-11932, 2012.

715 Browne, E. C., Wooldridge, P. J., Min, K. E., and Cohen, R. C.: On the role of monoterpene
716 chemistry in the remote continental boundary layer, Atmos. Chem. Phys., 14, 3, 1225-1238,
717 2014.

718 Camalier, L., Cox, W., and Dolwick, P.: The effects of meteorology on ozone in urban areas and
719 their use in assessing ozone trends, Atmos. Environ., 41, 33, 7127-7137, 2007.

720 Canty, T. P., Hembeck, L., Vinciguerra, T. P., Anderson, D. C., Goldberg, D. L., Carpenter, S. F.,
721 Allen, D. J., Loughner, C. P., Salawitch, R. J., and Dickerson, R. R.: Ozone and NOx chemistry
722 in the eastern US: evaluation of CMAQ/CB05 with satellite (OMI) data, Atmos. Chem. Phys., 15,
723 4, 4427-4461, 2015.

724 Cooper, O. R., Gao, R.-S., Tarasick, D., Leblanc, T., and Sweeney, C.: Long-term ozone trends
725 at rural ozone monitoring sites across the United States, 1990–2010, J. Geophys. Res., 117,
726 D22307, 2012.

727 Crounse, J. D., Paulot, F., Kjaergaard, H. G., and Wennberg, P. O.: Peroxy radical isomerization
728 in the oxidation of isoprene, Phys. Chem. Chem. Phys., 13, 30, 13607-13613, 2011.

729 Darer, A. I., Cole-Filipiak, N. C., O'Connor, A. E., and Elrod, M. J.: Formation and Stability of
730 Atmospherically Relevant Isoprene-Derived Organosulfates and Organonitrates, Environ. Sci.
731 Technol., 45, 5, 1895-1902, 2011.

732 Donner, L. J., Wyman, B. L., Hemler, R. S., Horowitz, L. W., Ming, Y., Zhao, M., Golaz, J.-C.,
733 Ginoux, P., Lin, S.-J., Schwarzkopf, M. D., Austin, J., Alaka, G., Cooke, W. F., Delworth, T. L.,
734 Freidenreich, S. M., Gordon, C. T., Griffies, S. M., Held, I. M., Hurlin, W. J., Klein, S. A.,
735 Knutson, T. R., Langenhorst, A. R., Lee, H.-C., Lin, Y., Magi, B. I., Malyshev, S. L., Milly, P. C.
736 D., Naik, V., Nath, M. J., Pincus, R., Ploshay, J. J., Ramaswamy, V., Seman, C. J., Shevliakova,
737 E., Sirutis, J. J., Stern, W. F., Stouffer, R. J., Wilson, R. J., Winton, M., Wittenberg, A. T., and
738 Zeng, F.: The Dynamical Core, Physical Parameterizations, and Basic Simulation Characteristics
739 of the Atmospheric Component AM3 of the GFDL Global Coupled Model CM3, J. Climate, 24,
740 13, 3484-3519, 2011.

741 Edwards, P. M., Aikin, K. C., Dube, W. P., Fry, J. L., Gilman, J. B., de Gouw, J. A., Graus, M.
742 G., Hanisco, T. F., Holloway, J., Hubler, G., Kaiser, J., Keutsch, F. N., Lerner, B. M., Neuman, J.
743 A., Parrish, D. D., Peischl, J., Pollack, I. B., Ravishankara, A. R., Roberts, J. M., Ryerson, T. B.,
744 Trainer, M., Veres, P. R., Wolfe, G. M., Warneke, C., and Brown, S. S.: Transition from high- to
745 low-NOx control of night-time oxidation in the southeastern US, Nature Geosci, 10, 7, 490-495,
746 2017.

747 Fang, Y., Fiore, A. M., Horowitz, L., Levy, H., Hu, Y., and Russell, A.: Sensitivity of the NOy
748 budget over the United States to anthropogenic and lightning NOx in summer, J. Geophys. Res.,
749 115, D18, 2010.

750 Fehsenfeld, F. C., Ancellet, G., Bates, T. S., Goldstein, A. H., Hardesty, R. M., Honrath, R., Law,
751 K. S., Lewis, A. C., Leaitch, R., McKeen, S., Meagher, J., Parrish, D. D., Pszenny, A. A. P.,
752 Russell, P. B., Schlager, H., Seinfeld, J., Talbot, R., and Zbinden, R.: International Consortium
753 for Atmospheric Research on Transport and Transformation (ICARTT): North America to
754 Europe—Overview of the 2004 summer field study, J. Geophys. Res., 111, D23S01, 2006.

755 Fiore, A. M., Horowitz, L. W., Purves, D. W., Levy, H., Evans, M. J., Wang, Y., Li, Q., and
756 Yantosca, R. M.: Evaluating the contribution of changes in isoprene emissions to surface ozone
757 trends over the eastern United States, J. Geophys. Res., 110, D12303, 2005.

758 Fiore, A. M., Dentener, F. J., Wild, O., Cuvelier, C., Schultz, M. G., Hess, P., Textor, C., Schulz,
759 M., Doherty, R. M., and Horowitz, L. W.: Multimodel estimates of intercontinental source‐
760 receptor relationships for ozone pollution, J. Geophys. Res., 114, D4, 83-84, 2009.

761 Fischer, E., Jacob, D. J., Yantosca, R. M., Sulprizio, M. P., Millet, D., Mao, J., Paulot, F., Singh,
762 H., Roiger, A., and Ries, L.: Atmospheric peroxyacetyl nitrate (PAN): a global budget and
763 source attribution, Atmos. Chem. Phys., 14, 5, 2679-2698, 2014.

764 Fisher, J. A., Jacob, D. J., Travis, K. R., Kim, P. S., Marais, E. A., Miller, C. C., Yu, K., Zhu, L.,
765 Yantosca, R. M., and Sulprizio, M. P.: Organic nitrate chemistry and its implications for nitrogen
766 budgets in an isoprene- and monoterpene-rich atmosphere: constraints from aircraft (SEAC4RS)
767 and ground-based (SOAS) observations in the Southeast US, Atmos. Chem. Phys., 16, 1, 1-38,
768 2016.

769 Fry, J. L., Kiendler-Scharr, A., Rollins, A. W., Wooldridge, P. J., Brown, S. S., Fuchs, H., Dubé,
770 W., Mensah, A., dal Maso, M., Tillmann, R., Dorn, H. P., Brauers, T., and Cohen, R. C.: Organic
771 nitrate and secondary organic aerosol yield from NO3 oxidation of β-pinene evaluated using a
772 gas-phase kinetics/aerosol partitioning model, Atmos. Chem. Phys., 9, 4, 1431-1449, 2009.

773 Fry, J. L., Draper, D. C., Barsanti, K. C., Smith, J. N., Ortega, J., Winkler, P. M., Lawler, M. J.,
774 Brown, S. S., Edwards, P. M., Cohen, R. C., and Lee, L.: Secondary Organic Aerosol Formation
775 and Organic Nitrate Yield from NO3 Oxidation of Biogenic Hydrocarbons, Environ. Sci.
776 Technol., 48, 20, 11944-11953, 2014.

777 Granier, C., Bessagnet, B., Bond, T., D'Angiola, A., Denier van der Gon, H., Frost, G. J., Heil,
778 A., Kaiser, J. W., Kinne, S., Klimont, Z., Kloster, S., Lamarque, J.-F., Liousse, C., Masui, T.,
779 Meleux, F., Mieville, A., Ohara, T., Raut, J.-C., Riahi, K., Schultz, M. G., Smith, S. J.,

780 Thompson, A., van Aardenne, J., van der Werf, G. R., and van Vuuren, D. P.: Evolution of
781 anthropogenic and biomass burning emissions of air pollutants at global and regional scales
782 during the 1980–2010 period, Clim. Change, 109, 1, 163-190, 2011.

783 Grimm, J. W., and Lynch, J. A.: Improved daily precipitation nitrate and ammonium
784 concentration models for the Chesapeake Bay Watershed, Environ. Pollut., 135, 3, 445-455,
785 2005.

786 Hardacre, C., Wild, O., and Emberson, L.: An evaluation of ozone dry deposition in global scale
787 chemistry climate models, Atmos. Chem. Phys., 15, 11, 6419-6436, 2015.

788 Henderson, B. H., Pinder, R. W., Crooks, J., Cohen, R. C., Hutzell, W. T., Sarwar, G., Goliff, W.
789 S., Stockwell, W. R., Fahr, A., Mathur, R., Carlton, A. G., and Vizuete, W.: Evaluation of
790 simulated photochemical partitioning of oxidized nitrogen in the upper troposphere, Atmos.
791 Chem. Phys., 11, 1, 275-291, 2011.

792 Hidy, G. M., Blanchard, C. L., Baumann, K., Edgerton, E., Tanenbaum, S., Shaw, S., Knipping,
793 E., Tombach, I., Jansen, J., and Walters, J.: Chemical climatology of the southeastern United
794 States, 1999-2013, Atmos. Chem. Phys., 14, 21, 11893-11914, 2014.

795 Hidy, G. M., and Blanchard, C. L.: Precursor reductions and ground-level ozone in the
796 Continental United States, J. Air Waste Manag. Assoc., 65, 10, 1261-1282, 2015.

797 Horowitz, L. W., Liang, J., Gardner, G. M., and Jacob, D. J.: Export of reactive nitrogen from
798 North America during summertime: Sensitivity to hydrocarbon chemistry, J. Geophys. Res., 103,
799 D11, 13451-13476, 1998.

800 Horowitz, L. W., Fiore, A. M., Milly, G. P., Cohen, R. C., Perring, A., Wooldridge, P. J., Hess, P.
801 G., Emmons, L. K., and Lamarque, J.-F.: Observational constraints on the chemistry of isoprene
802 nitrates over the eastern United States, J. Geophys. Res., 112, D12S08, 2007.

803 Hu, K. S., Darer, A. I., and Elrod, M. J.: Thermodynamics and kinetics of the hydrolysis of
804 atmospherically relevant organonitrates and organosulfates, Atmos. Chem. Phys., 11, 16, 8307-
805 8320, 2011.

806 Hudman, R., Jacob, D. J., Cooper, O., Evans, M., Heald, C., Park, R., Fehsenfeld, F., Flocke, F.,
807 Holloway, J., and Hübler, G.: Ozone production in transpacific Asian pollution plumes and
808 implications for ozone air quality in California, J. Geophys. Res., 109, D23, 2004.

809 Hudman, R. C., Jacob, D. J., Turquety, S., Leibensperger, E. M., Murray, L. T., Wu, S., Gilliland,
810 A. B., Avery, M., Bertram, T. H., Brune, W., Cohen, R. C., Dibb, J. E., Flocke, F. M., Fried, A.,
811 Holloway, J., Neuman, J. A., Orville, R., Perring, A., Ren, X., Sachse, G. W., Singh, H. B.,
812 Swanson, A., and Wooldridge, P. J.: Surface and lightning sources of nitrogen oxides over the
813 United States: Magnitudes, chemical evolution, and outflow, J. Geophys. Res., 112, D12S05,
814 2007.

815 Hudman, R. C., Murray, L. T., Jacob, D. J., Turquety, S., Wu, S., Millet, D. B., Avery, M.,
816 Goldstein, A. H., and Holloway, J.: North American influence on tropospheric ozone and the

817 effects of recent emission reductions: Constraints from ICARTT observations, J. Geophys. Res.,
818 114, D7, 2009.

819 Hudman, R. C., Moore, N. E., Mebust, A. K., Martin, R. V., Russell, A. R., Valin, L. C., and
820 Cohen, R. C.: Steps towards a mechanistic model of global soil nitric oxide emissions:
821 implementation and space based-constraints, Atmos. Chem. Phys., 12, 16, 7779-7795, 2012.

822 Ito, A., Sillman, S., and Penner, J. E.: Global chemical transport model study of ozone response
823 to changes in chemical kinetics and biogenic volatile organic compounds emissions due to
824 increasing temperatures: Sensitivities to isoprene nitrate chemistry and grid resolution, J.
825 Geophys. Res., 114, D09301, 2009.

826 Jacob, D. J., and Winner, D. A.: Effect of climate change on air quality, Atmos. Environ., 43, 1,
827 51-63, 2009.

828 Jacobs, M. I., Burke, W. J., and Elrod, M. J.: Kinetics of the reactions of isoprene-derived
829 hydroxynitrates: gas phase epoxide formation and solution phase hydrolysis, Atmos. Chem.
830 Phys., 14, 17, 8933-8946, 2014.

831 Jenkin, M. E., Young, J. C., and Rickard, A. R.: The MCM v3.3.1 degradation scheme for
832 isoprene, Atmos. Chem. Phys., 15, 20, 11433-11459, 2015.

833 Kavassalis, S., and Murphy, J. G.: Understanding ozone-meteorology correlations: a role for dry
834 deposition, Geophys. Res. Lett.10.1002/2016GL071791, 2017.

835 Krotkov, N. A., McLinden, C. A., Li, C., Lamsal, L. N., Celarier, E. A., Marchenko, S. V.,
836 Swartz, W. H., Bucsela, E. J., Joiner, J., Duncan, B. N., Boersma, K. F., Veefkind, J. P., Levelt,
837 P. F., Fioletov, V. E., Dickerson, R. R., He, H., Lu, Z., and Streets, D. G.: Aura OMI
838 observations of regional SO2 and NO2 pollution changes from 2005 to 2015, Atmos. Chem.
839 Phys., 16, 7, 4605-4629, 2016.

840 Lam, Y., Fu, J., Wu, S., and Mickley, L.: Impacts of future climate change and effects of
841 biogenic emissions on surface ozone and particulate matter concentrations in the United States,
842 Atmos. Chem. Phys., 11, 10, 4789-4806, 2011.

843 Lamarque, J.-F., Kyle, G. P., Meinshausen, M., Riahi, K., Smith, S. J., van Vuuren, D. P.,
844 Conley, A. J., and Vitt, F.: Global and regional evolution of short-lived radiatively-active gases
845 and aerosols in the Representative Concentration Pathways, Clim. Change, 109, 1, 191-212,
846 2011.

847 Lamsal, L. N., Duncan, B. N., Yoshida, Y., Krotkov, N. A., Pickering, K. E., Streets, D. G., and
848 Lu, Z.: U.S. NO2 trends (2005–2013): EPA Air Quality System (AQS) data versus improved
849 observations from the Ozone Monitoring Instrument (OMI), Atmos. Environ., 110, 130-143,
850 2015.

851 Lee, B. H., Mohr, C., Lopez-Hilfiker, F. D., Lutz, A., Hallquist, M., Lee, L., Romer, P., Cohen,
852 R. C., Iyer, S., Kurtén, T., Hu, W., Day, D. A., Campuzano-Jost, P., Jimenez, J. L., Xu, L., Ng, N.
853 L., Guo, H., Weber, R. J., Wild, R. J., Brown, S. S., Koss, A., de Gouw, J., Olson, K., Goldstein,

A. H., Seco, R., Kim, S., McAvey, K., Shepson, P. B., Starn, T., Baumann, K., Edgerton, E. S., Liu, J., Shilling, J. E., Miller, D. O., Brune, W., Schobesberger, S., D'Ambro, E. L., and Thornton, J. A.: Highly functionalized organic nitrates in the southeast United States: Contribution to secondary organic aerosol and reactive nitrogen budgets, Proc. Natl. Acad. Sci. U.S.A., 113, 6, 1516-1521, 2016.

Lee, L., Teng, A. P., Wennberg, P. O., Crounse, J. D., and Cohen, R. C.: On Rates and Mechanisms of OH and O3 Reactions with Isoprene-Derived Hydroxy Nitrates, J. Phys. Chem. A, 118, 9, 1622-1637, 2014.

Li, J., Mao, J., Min, K.-E., Washenfelder, R. A., Brown, S. S., Kaiser, J., Keutsch, F. N., Volkamer, R., Wolfe, G. M., Hanisco, T. F., Pollack, I. B., Ryerson, T. B., Graus, M., Gilman, J. B., Lerner, B. M., Warneke, C., de Gouw, J. A., Middlebrook, A. M., Liao, J., Welti, A., Henderson, B. H., McNeill, V. F., Hall, S. R., Ullmann, K., Donner, L. J., Paulot, F., and Horowitz, L. W.: Observational constraints on glyoxal production from isoprene oxidation and its contribution to organic aerosol over the Southeast United States, J. Geophys. Res., 121, 16, 2016JD025331, 2016.

Li, Q., Jacob, D. J., Munger, J. W., Yantosca, R. M., and Parrish, D. D.: Export of NOy from the North American boundary layer: Reconciling aircraft observations and global model budgets, J. Geophys. Res., 109, D2, 2004.

Liang, J., Horowitz, L. W., Jacob, D. J., Wang, Y., Fiore, A. M., Logan, J. A., Gardner, G. M., and Munger, J. W.: Seasonal budgets of reactive nitrogen species and ozone over the United States, and export fluxes to the global atmosphere, J. Geophys. Res., 103, D11, 13435-13450, 1998.

Lin, M., Horowitz, L. W., Payton, R., Fiore, A. M., and Tonnesen, G.: US surface ozone trends and extremes from 1980 to 2014: quantifying the roles of rising Asian emissions, domestic controls, wildfires, and climate, Atmos. Chem. Phys., 17, 4, 2943-2970, 2017.

Liu, X., Zhang, Y., Huey, L. G., Yokelson, R. J., Wang, Y., Jimenez, J. L., Campuzano-Jost, P., Beyersdorf, A. J., Blake, D. R., Choi, Y., St. Clair, J. M., Crounse, J. D., Day, D. A., Diskin, G. S., Fried, A., Hall, S. R., Hanisco, T. F., King, L. E., Meinardi, S., Mikoviny, T., Palm, B. B., Peischl, J., Perring, A. E., Pollack, I. B., Ryerson, T. B., Sachse, G., Schwarz, J. P., Simpson, I. J., Tanner, D. J., Thornhill, K. L., Ullmann, K., Weber, R. J., Wennberg, P. O., Wisthaler, A., Wolfe, G. M., and Ziemba, L. D.: Agricultural fires in the southeastern U.S. during SEAC4RS: Emissions of trace gases and particles and evolution of ozone, reactive nitrogen, and organic aerosol, J. Geophys. Res., 121, 12, 7383-7414, 2016.

Lockwood, A. L., Shepson, P. B., Fiddler, M. N., and Alaghmand, M.: Isoprene nitrates: preparation, separation, identification, yields, and atmospheric chemistry, Atmos. Chem. Phys., 10, 13, 6169-6178, 2010.

Lu, Z., Streets, D. G., De Foy, B., Lamsal, L. N., Duncan, B. N., and Xing, J.: Emissions of nitrogen oxides from US urban areas: estimation from Ozone Monitoring Instrument retrievals for 2005-2014, Atmos. Chem. Phys., 15, 10, 14961-15003, 2015.

893 Mao, J., Horowitz, L. W., Naik, V., Fan, S., Liu, J., and Fiore, A. M.: Sensitivity of tropospheric
894 oxidants to biomass burning emissions: implications for radiative forcing, Geophys. Res. Lett.,
895 40, 6, 1241-1246, 2013a.

896 Mao, J., Paulot, F., Jacob, D. J., Cohen, R. C., Crounse, J. D., Wennberg, P. O., Keller, C. A.,
897 Hudman, R. C., Barkley, M. P., and Horowitz, L. W.: Ozone and organic nitrates over the
898 eastern United States: Sensitivity to isoprene chemistry, J. Geophys. Res., 118, 19, 11,256-
899 211,268, 2013b.

900 Metcalfe, S. E., Whyatt, J. D., Nicholson, J. P. G., Derwent, R. G., and Heywood, E.: Issues in
901 model validation: assessing the performance of a regional-scale acid deposition model using
902 measured and modelled data, Atmos. Environ., 39, 4, 587-598, 2005.

903 Millet, D. B., Jacob, D. J., Boersma, K. F., Fu, T. M., Kurosu, T. P., Chance, K., Heald, C. L.,
904 and Guenther, A.: Spatial Distribution of Isoprene Emissions from North America Derived from
905 Dormaldehyde Column Measurements by the OMI Satellite Sensor, J. Geophys. Res., 113, D2,
906 194-204, 2008.

907 Miyazaki, K., Eskes, H., Sudo, K., Boersma, K. F., Bowman, K., and Kanaya, Y.: Decadal
908 changes in global surface NOx emissions from multi-constituent satellite data assimilation,
909 Atmos. Chem. Phys., 17, 2, 807-837, 2017.

910 Moxim, W., Levy, H., and Kasibhatla, P.: Simulated global tropospheric PAN: Its transport and
911 impact on NO x, J. Geophys. Res., 101, D7, 12621-12638, 1996.

912 Müller, J. F., Peeters, J., and Stavrakou, T.: Fast photolysis of carbonyl nitrates from isoprene,
913 Atmos. Chem. Phys., 14, 5, 2497-2508, 2014.

914 Nah, T., Sanchez, J., Boyd, C. M., and Ng, N. L.: Photochemical Aging of α-pinene and β-pinene
915 Secondary Organic Aerosol formed from Nitrate Radical Oxidation, Environ. Sci. Technol., 50,
916 1, 222-231, 2016.

917 Naik, V., Horowitz, L. W., Fiore, A. M., Ginoux, P., Mao, J., Aghedo, A. M., and Levy, H.:
918 Impact of preindustrial to present-day changes in short-lived pollutant emissions on atmospheric
919 composition and climate forcing, J. Geophys. Res., 118, 14, 8086-8110, 2013.

920 Neuman, J., Parrish, D., Trainer, M., Ryerson, T., Holloway, J., Nowak, J., Swanson, A., Flocke,
921 F., Roberts, J., and Brown, S.: Reactive nitrogen transport and photochemistry in urban plumes
922 over the North Atlantic Ocean, J. Geophys. Res., 111, D23, 2006.

923 Ng, N. L., Kwan, A. J., Surratt, J. D., Chan, A. W. H., Chhabra, P. S., Sorooshian, A., Pye, H. O.
924 T., Crounse, J. D., Wennberg, P. O., Flagan, R. C., and Seinfeld, J. H.: Secondary organic
925 aerosol (SOA) formation from reaction of isoprene with nitrate radicals (NO3), Atmos. Chem.
926 Phys., 8, 14, 4117-4140, 2008.

927 Ng, N. L., Brown, S. S., Archibald, A. T., Atlas, E., Cohen, R. C., Crowley, J. N., Day, D. A.,
928 Donahue, N. M., Fry, J. L., Fuchs, H., Griffin, R. J., Guzman, M. I., Herrmann, H., Hodzic, A.,
929 Iinuma, Y., Jimenez, J. L., Kiendler-Scharr, A., Lee, B. H., Luecken, D. J., Mao, J., McLaren, R.,

Mutzel, A., Osthoff, H. D., Ouyang, B., Picquet-Varrault, B., Platt, U., Pye, H. O. T., Rudich, Y., Schwantes, R. H., Shiraiwa, M., Stutz, J., Thornton, J. A., Tilgner, A., Williams, B. J., and Zaveri, R. A.: Nitrate radicals and biogenic volatile organic compounds: oxidation, mechanisms, and organic aerosol, Atmos. Chem. Phys., 17, 3, 2103-2162, 2017.

Nguyen, T. B., Crounse, J. D., Teng, A. P., St. Clair, J. M., Paulot, F., Wolfe, G. M., and Wennberg, P. O.: Rapid deposition of oxidized biogenic compounds to a temperate forest, Proc. Natl. Acad. Sci. U.S.A., 112, 5, E392-E401, 2015.

Nozière, B., Barnes, I., and Becker, K. H.: Product study and mechanisms of the reactions of α‐pinene and of pinonaldehyde with OH radicals, J. Geophys. Res., 104, D19, 23645-23656, 1999.

Ott, L. E., Pickering, K. E., Stenchikov, G. L., Allen, D. J., DeCaria, A. J., Ridley, B., Lin, R.-F., Lang, S., and Tao, W.-K.: Production of lightning NOx and its vertical distribution calculated from three-dimensional cloud-scale chemical transport model simulations, J. Geophys. Res., 115, D4, 2010.

Parrish, D., Ryerson, T., Holloway, J., Neuman, J., Roberts, J., Williams, J., Stroud, C., Frost, G., Trainer, M., and Hübler, G.: Fraction and composition of NOy transported in air masses lofted from the North American continental boundary layer, J. Geophys. Res., 109, D9, 2004.

Paulot, F., Crounse, J. D., Kjaergaard, H. G., Kroll, J. H., Seinfeld, J. H., and Wennberg, P. O.: Isoprene photooxidation: new insights into the production of acids and organic nitrates, Atmos. Chem. Phys., 9, 4, 1479-1501, 2009.

Paulot, F., Henze, D. K., and Wennberg, P. O.: Impact of the isoprene photochemical cascade on tropical ozone, Atmos. Chem. Phys., 12, 3, 1307-1325, 2012.

Paulot, F., Jacob, D. J., Pinder, R. W., Bash, J. O., Travis, K., and Henze, D. K.: Ammonia emissions in the United States, European Union, and China derived by high-resolution inversion of ammonium wet deposition data: Interpretation with a new agricultural emissions inventory (MASAGE_NH3), J. Geophys. Res., 119, 7, 4343-4364, 2014.

Paulot, F., Ginoux, P., Cooke, W. F., Donner, L. J., Fan, S., Lin, M. Y., Mao, J., Naik, V., and Horowitz, L. W.: Sensitivity of nitrate aerosols to ammonia emissions and to nitrate chemistry: implications for present and future nitrate optical depth, Atmos. Chem. Phys., 16, 3, 1459-1477, 2016.

Peeters, J., Müller, J.-F., Stavrakou, T., and Nguyen, V. S.: Hydroxyl Radical Recycling in Isoprene Oxidation Driven by Hydrogen Bonding and Hydrogen Tunneling: The Upgraded LIM1 Mechanism, J. Phys. Chem. A, 118, 38, 8625-8643, 2014.

Perring, A. E., Bertram, T. H., Wooldridge, P. J., Fried, A., Heikes, B. G., Dibb, J., Crounse, J. D., Wennberg, P. O., Blake, N. J., Blake, D. R., Brune, W. H., Singh, H. B., and Cohen, R. C.: Airborne observations of total RONO2: new constraints on the yield and lifetime of isoprene nitrates, Atmos. Chem. Phys., 9, 4, 1451-1463, 2009.

967 Perring, A. E., Pusede, S. E., and Cohen, R. C.: An Observational Perspective on the
968 Atmospheric Impacts of Alkyl and Multifunctional Nitrates on Ozone and Secondary Organic
969 Aerosol, Chem. Rev., 113, 8, 5848-5870, 2013.

970 Philip, S., Martin, R. V., and Keller, C. A.: Sensitivity of chemistry-transport model simulations
971 to the duration of chemical and transport operators: a case study with GEOS-Chem v10-01,
972 Geosci. Model Dev., 9, 5, 1683-1695, 2016.

973 Pickering, K. E., Wang, Y., Tao, W. K., Price, C., and Müller, J. F.: Vertical distributions of
974 lightning NOx for use in regional and global chemical transport models, J. Geophys. Res., 103,
975 D23, 31203–31216, 1998.

976 Pierce, R. B., Schaack, T., Al-Saadi, J. A., Fairlie, T. D., Kittaka, C., Lingenfelser, G., Natarajan,
977 M., Olson, J., Soja, A., Zapotocny, T., Lenzen, A., Stobie, J., Johnson, D., Avery, M. A., Sachse,
978 G. W., Thompson, A., Cohen, R., Dibb, J. E., Crawford, J., Rault, D., Martin, R., Szykman, J.,
979 and Fishman, J.: Chemical data assimilation estimates of continental U.S. ozone and nitrogen
980 budgets during the Intercontinental Chemical Transport Experiment–North America, J. Geophys.
981 Res., 112, D12, 2007.

982 Pollack, I. B., Ryerson, T. B., Trainer, M., Neuman, J., Roberts, J. M., and Parrish, D. D.: Trends
983 in ozone, its precursors, and related secondary oxidation products in Los Angeles, California: A
984 synthesis of measurements from 1960 to 2010, J. Geophys. Res., 118, 11, 5893-5911, 2013.

985 Praske, E., Crounse, J. D., Bates, K. H., Kurtén, T., Kjaergaard, H. G., and Wennberg, P. O.:
986 Atmospheric Fate of Methyl Vinyl Ketone: Peroxy Radical Reactions with NO and HO2, J. Phys.
987 Chem. A, 119, 19, 4562-4572, 2015.

988 Pye, H. O. T., Luecken, D. J., Xu, L., Boyd, C. M., Ng, N. L., Baker, K. R., Ayres, B. R., Bash, J.
989 O., Baumann, K., Carter, W. P. L., Edgerton, E., Fry, J. L., Hutzell, W. T., Schwede, D. B., and
990 Shepson, P. B.: Modeling the Current and Future Roles of Particulate Organic Nitrates in the
991 Southeastern United States, Environ. Sci. Technol., 49, 24, 14195-14203, 2015.

992 Rieder, H. E., Fiore, A. M., Horowitz, L. W., and Naik, V.: Projecting policy‐relevant metrics
993 for high summertime ozone pollution events over the eastern United States due to climate and
994 emission changes during the 21st century, J. Geophys. Res., 120, 2, 784-800, 2015.

995 Rindelaub, J. D., McAvey, K. M., and Shepson, P. B.: The photochemical production of organic
996 nitrates from α-pinene and loss via acid-dependent particle phase hydrolysis, Atmos. Environ.,
997 100, 193-201, 2015.

998 Rindelaub, J. D., Borca, C. H., Hostetler, M. A., Slade, J. H., Lipton, M. A., Slipchenko, L. V.,
999 and Shepson, P. B.: The acid-catalyzed hydrolysis of an α-pinene-derived organic nitrate:
1000 kinetics, products, reaction mechanisms, and atmospheric impact, Atmos. Chem. Phys., 16, 23,
1001 15425-15432, 2016.

1002 Rollins, A. W., Kiendler-Scharr, A., Fry, J. L., Brauers, T., Brown, S. S., Dorn, H. P., Dubé, W.
1003 P., Fuchs, H., Mensah, A., Mentel, T. F., Rohrer, F., Tillmann, R., Wegener, R., Wooldridge, P.

J., and Cohen, R. C.: Isoprene oxidation by nitrate radical: alkyl nitrate and secondary organic aerosol yields, Atmos. Chem. Phys., 9, 18, 6685-6703, 2009.

Rollins, A. W., Smith, J. D., Wilson, K. R., and Cohen, R. C.: Real Time In Situ Detection of Organic Nitrates in Atmospheric Aerosols, Environ. Sci. Technol., 44, 14, 5540-5545, 2010.

Romer, P. S., Duffey, K. C., Wooldridge, P. J., Allen, H. M., Ayres, B. R., Brown, S. S., Brune, W. H., Crounse, J. D., de Gouw, J., Draper, D. C., Feiner, P. A., Fry, J. L., Goldstein, A. H., Koss, A., Misztal, P. K., Nguyen, T. B., Olson, K., Teng, A. P., Wennberg, P. O., Wild, R. J., Zhang, L., and Cohen, R. C.: The lifetime of nitrogen oxides in an isoprene-dominated forest, Atmos. Chem. Phys., 16, 12, 7623-7637, 2016.

Russell, A. R., Valin, L. C., and Cohen, R. C.: Trends in OMI NO2 observations over the United States: effects of emission control technology and the economic recession, Atmos. Chem. Phys., 12, 24, 12197-12209, 2012.

Sanderson, M., Dentener, F., Fiore, A., Cuvelier, C., Keating, T., Zuber, A., Atherton, C., Bergmann, D., Diehl, T., and Doherty, R.: A multi‐model study of the hemispheric transport and deposition of oxidised nitrogen, Geophys. Res. Lett., 35, 17, 2008.

Sato, K.: Detection of nitrooxypolyols in secondary organic aerosol formed from the photooxidation of conjugated dienes under high-NOx conditions, Atmos. Environ., 42, 28, 6851-6861, 2008.

Schwantes, R. H., Teng, A. P., Nguyen, T. B., Coggon, M. M., Crounse, J. D., St. Clair, J. M., Zhang, X., Schilling, K. A., Seinfeld, J. H., and Wennberg, P. O.: Isoprene NO3 Oxidation Products from the RO2 + HO2 Pathway, J. Phys. Chem. A, 119, 40, 10158-10171, 2015.

Sillman, S.: Ozone production efficiency and loss of NO x in power plant plumes: Photochemical model and interpretation of measurements in Tennessee, J. Geophys. Res., 105, D7, 9189-9202, 2000.

Simon, H., Reff, A., Wells, B., Xing, J., and Frank, N.: Ozone Trends Across the United States over a Period of Decreasing NOx and VOC Emissions, Environ. Sci. Technol., 49, 1, 186-195, 2015.

Singh, H. B., Brune, W. H., Crawford, J. H., Jacob, D. J., and Russell, P. B.: Overview of the summer 2004 Intercontinental Chemical Transport Experiment–North America (INTEX-A), J. Geophys. Res., 111, D24S01, 2006.

Singh, H. B., Salas, L., Herlth, D., Kolyer, R., Czech, E., Avery, M., Crawford, J. H., Pierce, R. B., Sachse, G. W., Blake, D. R., Cohen, R. C., Bertram, T. H., Perring, A., Wooldridge, P. J., Dibb, J., Huey, G., Hudman, R. C., Turquety, S., Emmons, L. K., Flocke, F., Tang, Y., Carmichael, G. R., and Horowitz, L. W.: Reactive nitrogen distribution and partitioning in the North American troposphere and lowermost stratosphere, J. Geophys. Res., 112, D12, 2007.

1039 Spittler, M., Barnes, I., Bejan, I., Brockmann, K. J., Benter, T., and Wirtz, K.: Reactions of NO3
1040 radicals with limonene and α-pinene: Product and SOA formation, Atmos. Environ., 40, 116-127,
1041 2006.

1042 St. Clair, J. M., Rivera-Rios, J. C., Crounse, J. D., Knap, H. C., Bates, K. H., Teng, A. P.,
1043 Jørgensen, S., Kjaergaard, H. G., Keutsch, F. N., and Wennberg, P. O.: Kinetics and Products of
1044 the Reaction of the First-Generation Isoprene Hydroxy Hydroperoxide (ISOPOOH) with OH, J.
1045 Phys. Chem. A, 120, 9, 1441-1451, 2016.

1046 Steiner, A. L., Davis, A. J., Sillman, S., Owen, R. C., Michalak, A. M., and Fiore, A. M.:
1047 Observed suppression of ozone formation at extremely high temperatures due to chemical and
1048 biophysical feedbacks, Proc. Natl. Acad. Sci. U.S.A., 107, 46, 19685-19690, 2010.

1049 Stoeckenius, T. E., Hogrefe, C., Zagunis, J., Sturtz, T. M., Wells, B., and Sakulyanontvittaya, T.:
1050 A comparison between 2010 and 2006 air quality and meteorological conditions, and emissions
1051 and boundary conditions used in simulations of the AQMEII-2 North American domain, Atmos.
1052 Environ., 115, 389-403, 2015.

1053 Stohl, A., Trainer, M., Ryerson, T. B., Holloway, J. S., and Parrish, D. D.: Export of NOy from
1054 the North American boundary layer during 1996 and 1997 North Atlantic Regional Experiments,
1055 J. Geophys. Res., 107, D11, ACH 11-11-ACH 11-13, 2002.

1056 Strode, S. A., Rodriguez, J. M., Logan, J. A., Cooper, O. R., Witte, J. C., Lamsal, L. N., Damon,
1057 M., Van Aartsen, B., Steenrod, S. D., and Strahan, S. E.: Trends and variability in surface ozone
1058 over the United States, J. Geophys. Res., 120, 17, 9020-9042, 2015.

1059 Szmigielski, R., Vermeylen, R., Dommen, J., Metzger, A., Maenhaut, W., Baltensperger, U., and
1060 Claeys, M.: The acid effect in the formation of 2-methyltetrols from the photooxidation of
1061 isoprene in the presence of NOx, Atmos. Res., 98, 2–4, 183-189, 2010.

1062 Tawfik, A. B., and Steiner, A. L.: A proposed physical mechanism for ozone-meteorology
1063 correlations using land–atmosphere coupling regimes, Atmos. Environ., 72, 50-59, 2013.

1064 Teng, A., Crounse, J., Lee, L., St Clair, J., Cohen, R., and Wennberg, P.: Hydroxy nitrate
1065 production in the OH-initiated oxidation of alkenes, Atmos. Chem. Phys., 15, 8, 4297-4316,
1066 2015.

1067 Tong, D. Q., Lamsal, L., Pan, L., Ding, C., Kim, H., Lee, P., Chai, T., Pickering, K. E., and
1068 Stajner, I.: Long-term NOx trends over large cities in the United States during the great recession:
1069 Comparison of satellite retrievals, ground observations, and emission inventories, Atmos.
1070 Environ., 107, 70-84, 2015.

1071 Toon, O. B., Maring, H., Dibb, J., Ferrare, R., Jacob, D. J., Jensen, E. J., Luo, Z. J., Mace, G. G.,
1072 Pan, L. L., Pfister, L., Rosenlof, K. H., Redemann, J., Reid, J. S., Singh, H. B., Thompson, A. M.,
1073 Yokelson, R., Minnis, P., Chen, G., Jucks, K. W., and Pszenny, A.: Planning, implementation
1074 and scientific goals of the Studies of Emissions and Atmospheric Composition, Clouds and
1075 Climate Coupling by Regional Surveys (SEAC4RS) field mission, J. Geophys. Res., 121, 4967-
1076 5009, 2016.

1077   Tost, H., Jöckel, P., Kerkweg, A., Pozzer, A., Sander, R., and Lelieveld, J.: Global cloud and
1078   precipitation chemistry and wet deposition: tropospheric model simulations with
1079   ECHAM5/MESSy1, Atmos. Chem. Phys., 7, 10, 2733-2757, 2007.

1080   Trainer, M., Parrish, D. D., Goldan, P. D., Roberts, J., and Fehsenfeld, F. C.: Review of
1081   observation-based analysis of the regional factors influencing ozone concentrations, Atmos.
1082   Environ., 34, 12–14, 2045-2061, 2000.

1083   Travis, K. R., Jacob, D. J., Fisher, J. A., Kim, P. S., Marais, E. A., Zhu, L., Yu, K., Miller, C. C.,
1084   Yantosca, R. M., Sulprizio, M. P., Thompson, A. M., Wennberg, P. O., Crounse, J. D., St. Clair,
1085   J. M., Cohen, R. C., Laughner, J. L., Dibb, J. E., Hall, S. R., Ullmann, K., Wolfe, G. M., Pollack,
1086   I. B., Peischl, J., Neuman, J. A., and Zhou, X.: Why do models overestimate surface ozone in the
1087   Southeast United States?, Atmos. Chem. Phys., 16, 21, 13561-13577, 2016.

1088   Val Martin, M., Heald, C. L., and Arnold, S. R.: Coupling dry deposition to vegetation
1089   phenology in the Community Earth System Model: Implications for the simulation of surface O
1090   3, Geophys. Res. Lett., 41, 8, 2988–2996, 2014.

1091   Warneke, C., Trainer, M., de Gouw, J. A., Parrish, D. D., Fahey, D. W., Ravishankara, A. R.,
1092   Middlebrook, A. M., Brock, C. A., Roberts, J. M., Brown, S. S., Neuman, J. A., Lerner, B. M.,
1093   Lack, D., Law, D., Hübler, G., Pollack, I., Sjostedt, S., Ryerson, T. B., Gilman, J. B., Liao, J.,
1094   Holloway, J., Peischl, J., Nowak, J. B., Aikin, K. C., Min, K. E., Washenfelder, R. A., Graus, M.
1095   G., Richardson, M., Markovic, M. Z., Wagner, N. L., Welti, A., Veres, P. R., Edwards, P.,
1096   Schwarz, J. P., Gordon, T., Dube, W. P., McKeen, S. A., Brioude, J., Ahmadov, R., Bougiatioti,
1097   A., Lin, J. J., Nenes, A., Wolfe, G. M., Hanisco, T. F., Lee, B. H., Lopez-Hilfiker, F. D.,
1098   Thornton, J. A., Keutsch, F. N., Kaiser, J., Mao, J., and Hatch, C. D.: Instrumentation and
1099   measurement strategy for the NOAA SENEX aircraft campaign as part of the Southeast
1100   Atmosphere Study 2013, Atmos. Meas. Tech., 9, 7, 3063-3093, 2016.

1101   Wolfe, G., Hanisco, T., Arkinson, H., Bui, T., Crounse, J., Dean‐Day, J., Goldstein, A.,
1102   Guenther, A., Hall, S., and Huey, G.: Quantifying sources and sinks of reactive gases in the
1103   lower atmosphere using airborne flux observations, Geophys. Res. Lett., 42, 19, 8231-8240,
1104   2015.

1105   Wu, S., Mickley, L. J., Jacob, D. J., Rind, D., and Streets, D. G.: Effects of 2000–2050 changes
1106   in climate and emissions on global tropospheric ozone and the policy-relevant background
1107   surface ozone in the United States, J. Geophys. Res., 113, D18312, 2008.

1108   Xing, J., Mathur, R., Pleim, J., Hogrefe, C., Gan, C. M., Wong, D. C., Wei, C., Gilliam, R., and
1109   Pouliot, G.: Observations and modeling of air quality trends over 1990–2010 across the Northern
1110   Hemisphere: China, the United States and Europe, Atmos. Chem. Phys., 15, 5, 2723-2747, 2015.

1111   Xiong, F., McAvey, K. M., Pratt, K. A., Groff, C. J., Hostetler, M. A., Lipton, M. A., Starn, T.
1112   K., Seeley, J. V., Bertman, S. B., Teng, A. P., Crounse, J. D., Nguyen, T. B., Wennberg, P. O.,
1113   Misztal, P. K., Goldstein, A. H., Guenther, A. B., Koss, A. R., Olson, K. F., de Gouw, J. A.,
1114   Baumann, K., Edgerton, E. S., Feiner, P. A., Zhang, L., Miller, D. O., Brune, W. H., and

1115 Shepson, P. B.: Observation of isoprene hydroxynitrates in the southeastern United States and
1116 implications for the fate of NOx, Atmos. Chem. Phys., 15, 19, 11257-11272, 2015.

1117 Xiong, F., Borca, C. H., Slipchenko, L. V., and Shepson, P. B.: Photochemical degradation of
1118 isoprene-derived 4,1-nitrooxy enal, Atmos. Chem. Phys., 16, 9, 5595-5610, 2016.

1119 Xu, L., Suresh, S., Guo, H., Weber, R. J., and Ng, N. L.: Aerosol characterization over the
1120 southeastern United States using high-resolution aerosol mass spectrometry: spatial and seasonal
1121 variation of aerosol composition and sources with a focus on organic nitrates, Atmos. Chem.
1122 Phys., 15, 13, 7307-7336, 2015.

1123 Yahya, K., Wang, K., Campbell, P., Glotfelty, T., He, J., and Zhang, Y.: Decadal evaluation of
1124 regional climate, air quality, and their interactions over the continental US and their interactions
1125 using WRF/Chem version 3.6.1, Geosci. Model Dev., 9, 2, 671-695, 2016.

1126 Yienger, J. J., and Levy, H. I.: Empirical model of soil-biogenic NOx emissions, J. Geophys.
1127 Res., 1001, D6, 11447-11464, 1995.

1128 Yu, K., Jacob, D. J., Fisher, J. A., Kim, P. S., Marais, E. A., Miller, C. C., Travis, K. R., Zhu, L.,
1129 Yantosca, R. M., Sulprizio, M. P., Cohen, R. C., Dibb, J. E., Fried, A., Mikoviny, T., Ryerson, T.
1130 B., Wennberg, P. O., and Wisthaler, A.: Sensitivity to grid resolution in the ability of a chemical
1131 transport model to simulate observed oxidant chemistry under high-isoprene conditions, Atmos.
1132 Chem. Phys., 16, 7, 4369-4378, 2016.
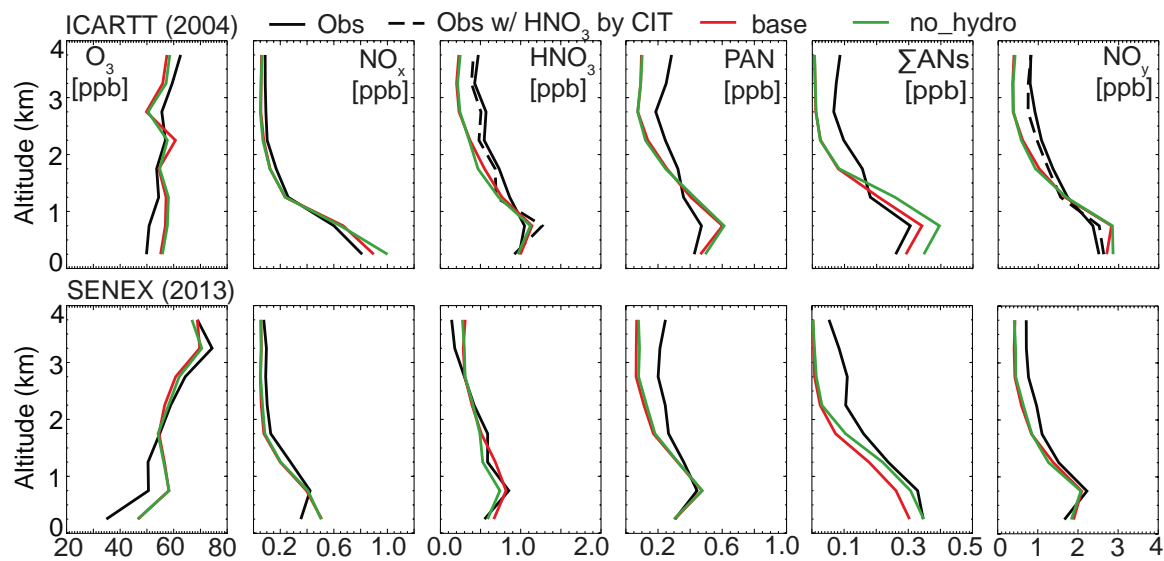
Figure 1. Mean vertical profiles of ozone and reactive oxidized nitrogen from observations during ICARTT (top row) and SENEX (bottom row) over SEUS (25 - 40° N, 100 - 75° W) during daytime, and model estimates from AM3 with hydrolysis of ISOPNB (red) and AM3 without hydrolysis of alkyl nitrates (green). The solid and dashed black lines in the HNO_3 of ICARTT represent measurements collected using mist chamber/IC by University of New Hampshire (UNH) and Chemical Ionization Mass Spectrometer by California Institute of Technology (CIT), respectively. NO_y from ICARTT is calculated as the sum of NO_x, HNO_3 (w/ UNH in the solid line and w/ CIT in the dashed line), PAN and total alkyl nitrates ($\sum$ANs). $\sum$ANs in the bottom row are from SEAC[4]RS.
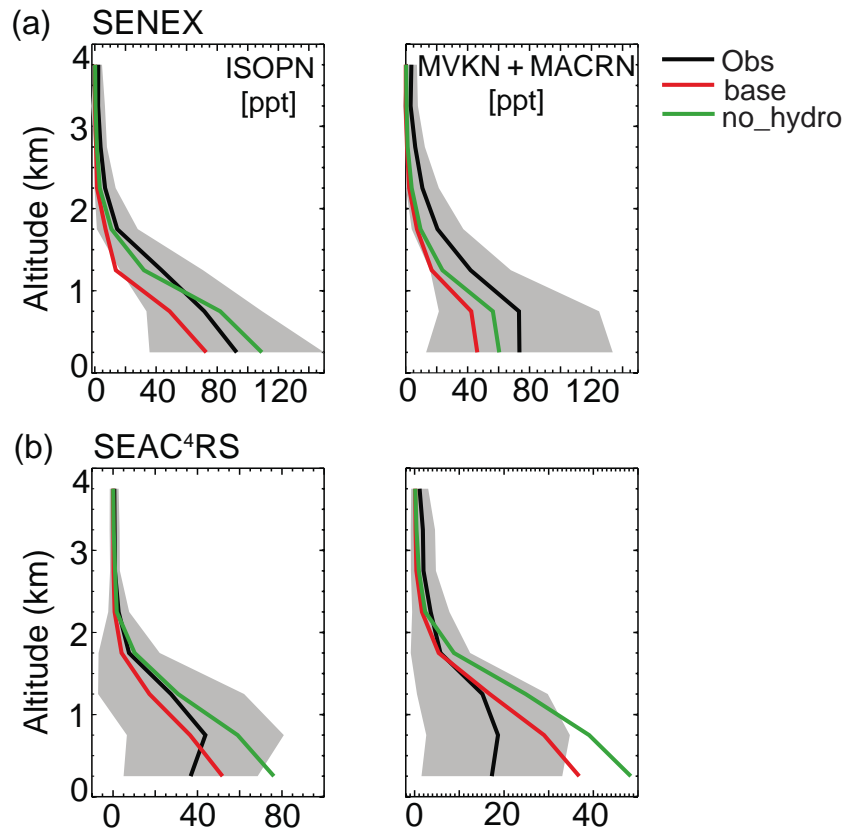
1143

Figure 2. Mean vertical profiles of ISOPN and MVNK+MACRN during (a) SENEX and (b) SEAC[4]RS over SEUS (25 - 40° N, 100 - 75° W). Black lines are the mean of observations. Red and green lines are the mean of modeled results with hydrolysis of ISOPNB and without hydrolysis of alkyl nitrates respectively. Grey shades are the one standard deviation (±σ) of averaged profiles of the measured tracers.
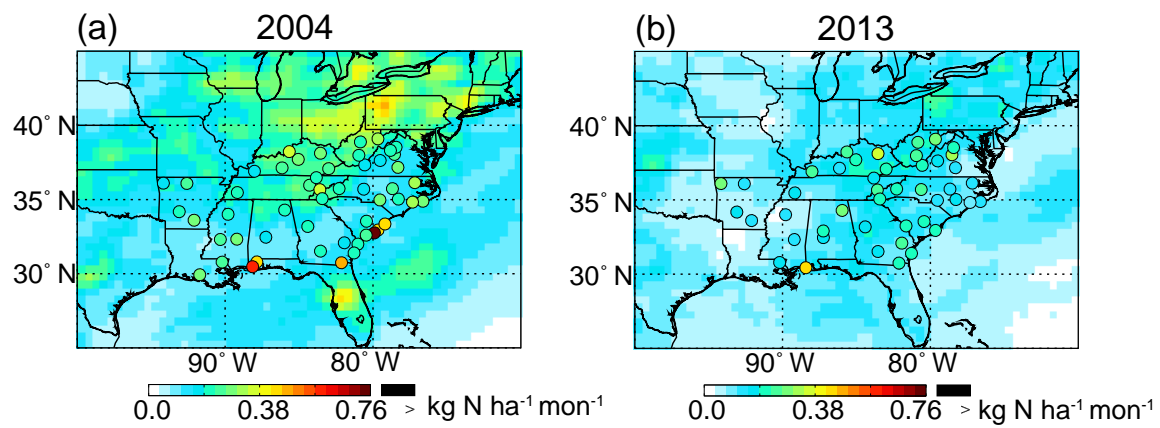
1149

1150 **Figure 3.** Nitrate wet deposition flux (kg N ha^{-1} mon^{-1}) from NADP (circles) and AM3
1151 (background) during July - August of 2004 and 2013.
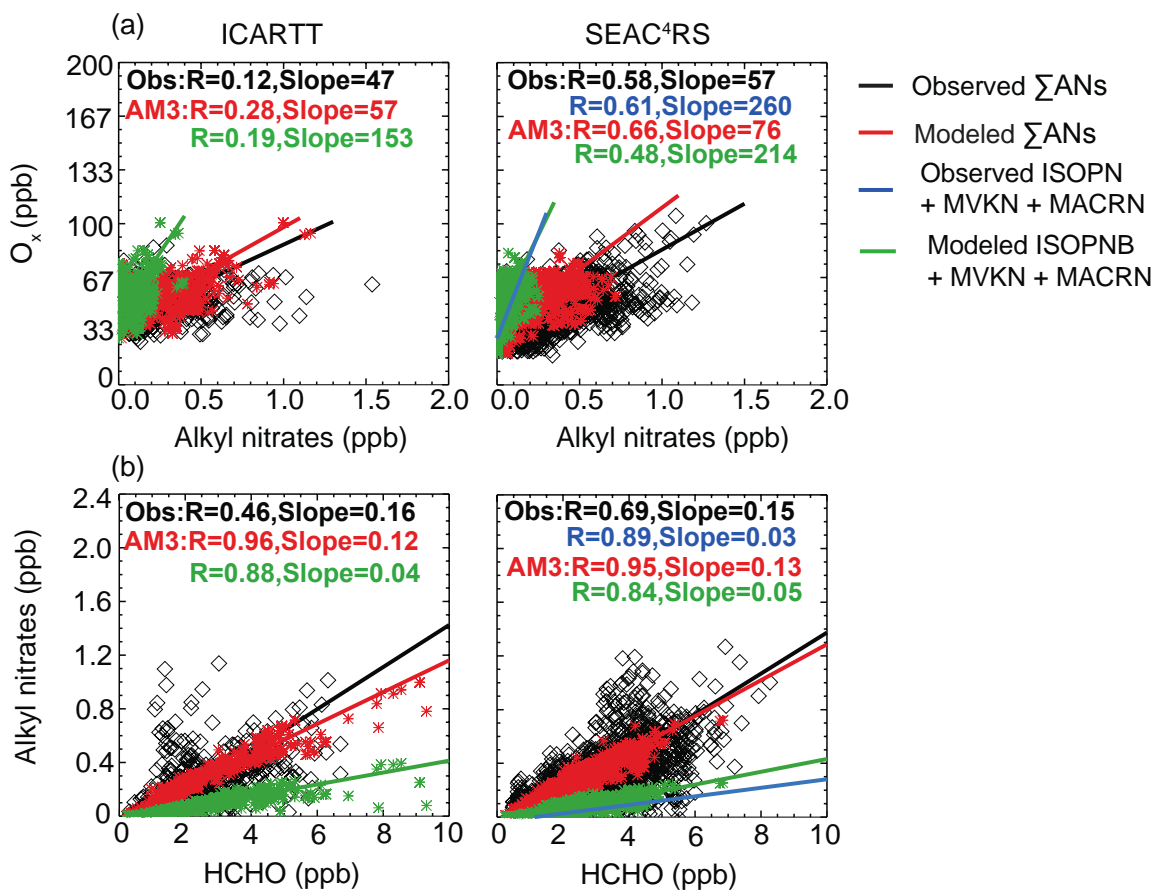
1152

Figure 4. O_x versus $\sum$ANs correlation (top; (a)) and $\sum$ANs versus formaldehyde correlation (bottom; (b)) within the boundary layer (< 1.5 km) during ICARTT (left) and SEAC⁴RS (right). Observations are in black diamonds; model estimates from AM3 with ISOPNB hydrolysis are in red symbols. Green symbols represent the correlation using modeled ISOPN + MVKN + MACRN. Blue symbols represent the correlation using observed ISOPN + MVKN + MACRN from SEAC⁴RS. Solid lines are the reduced major axis regression lines.
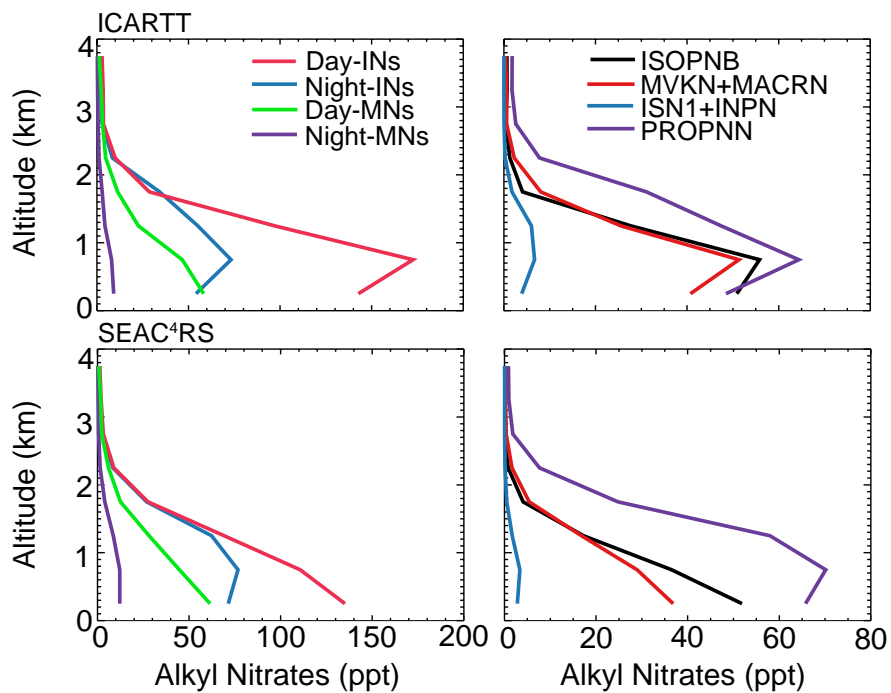
1159

1160 **Figure 5.** Mean vertical profiles of modeled alkyl nitrates from isoprene and monoterpene
1161 oxidation (left) and major isoprene nitrate species (right) during ICARTT (top row) and
1162 SEAC⁴RS (bottom row) from AM3 with hydrolysis of ISOPNB.
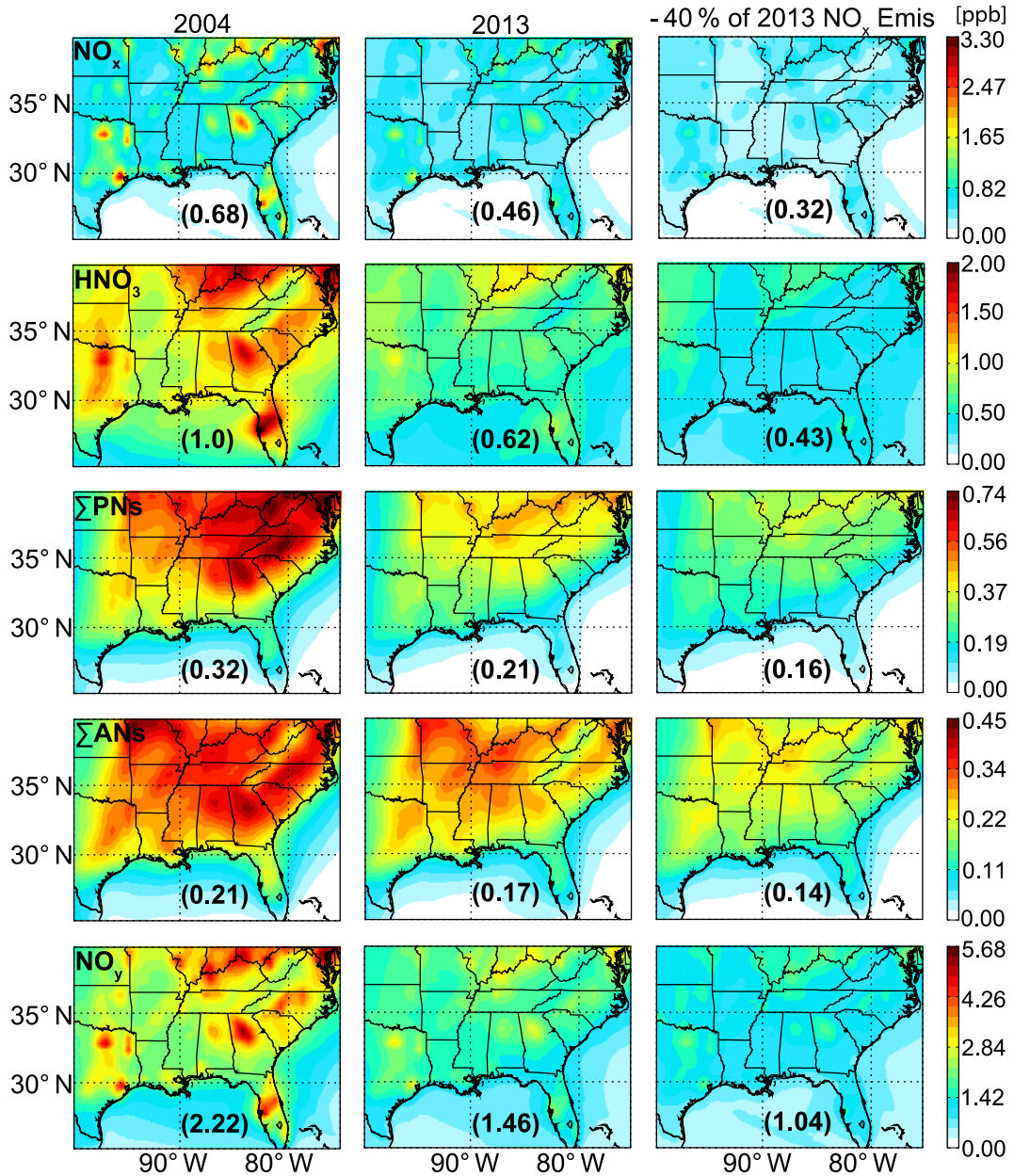
1163

Figure 6. Modeled mean NO_x, HNO_3, total peroxy nitrates (ΣPNs), total alkyl nitrates (ΣANs) and NO_y averaged over the boundary layer (< 1.5 km) of the Southeast U.S. during July - August of 2004 (left), 2013 (middle), and a scenario assuming 40 % reduction of 2013 anthropogenic NO_x emissions (right). Numbers in parentheses indicate mean concentrations over the plotted region. Note different color scales represent the concentration of each species.
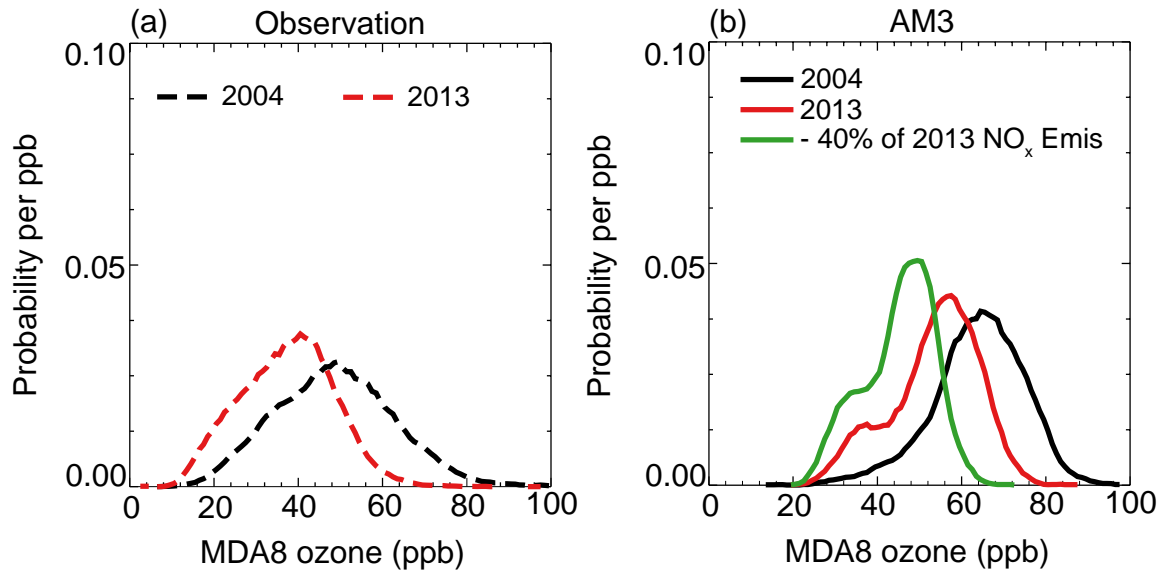
1169
1170   **Figure 7.** Observed (a) and simulated (b) probability density function of MDA8 ozone at AQS
1171   monitoring sites in Figure S3 during summer of 2004, 2013, and a scenario with 40 % reduction
1172   in the anthropogenic NO$_x$ emissions of 2013.

1173

1174 **Table 1.** Monthly averaged NO_x emissions in July-August of 2004 and 2013 over North America
1175 (25-50° N, 130-70° W) and over the Southeast US (25-40° N, 100-75° W) in brackets in AM3.

Source Type	2004 (Tg N)	2013 (Tg N)
Anthropogenic	0.42 (0.19)	0.25 (0.11)
Biomass Burning	8.4×10^{-3} (2.8×10^{-3})	8.4×10^{-3} (2.8×10^{-3})
Soils	2.9×10^{-2} (9.5×10^{-3})	2.9×10^{-2} (9.5×10^{-3})
Aircraft	8.8×10^{-3} (2.9×10^{-3})	8.0×10^{-3} (2.8×10^{-3})
Lightning	0.02 (0.01)	0.02 (0.01)
Total	0.49 (0.22)	0.32 (0.14)

1176

1177   **Table 2**. Case descriptions

Case name	Heterogeneous Loss of organic nitrates	NO$_x$ emissions	Meteorology
base	ISOPNB with a γ of 0.005 and followed by a hydrolysis rate of 9.26×10^{-5} s^{-1}	2004 and 2013	2004 and 2013
no_hydro	—	2004 and 2013	2004 and 2013
hydro_full	ISOPNB and DHDN with a γ of 0.005 and followed by a hydrolysis rate of 9.26×10^{-5} s^{-1}; TERPN1 with a γ of 0.01 and followed by a hydrolysis rate of 9.26×10^{-5} s^{-1}	2004 and 2013	2004 and 2013
hypo	Same with the base case	40 % reduction of NO$_x$ emissions of 2013	2013

Table 3. Monthly NO_y budget in the boundary layer (< 1.5 km) of the Southeast United States for July-August of 2004, 2013 and a scenario with 40 % reduction of anthropogenic NO_x emissions of 2013[a].

Species	2004					2013					- 40 % of 2013 Anthropogenic NO_x Emis				
	Emission	Chem (P-L)	Dry Dep	Wet Dep	Net Export	Emission	Chem (P-L)	Dry Dep	Wet Dep	Net Export	Emission	Chem (P-L)	Dry Dep	Wet Dep	Net Export
NO_x	208.7	-172.4	21.8	−	14.5	132.6	-105	14.2	−	13.4	88.3	-69.6	9.2	–	9.5
$\sum PNs$[b]		15.2	5.7	−	9.5		10.3	3.9	−	6.4		7.7	3.0	–	4.7
$\sum ANs$		24.3	14.3	6.2	3.8		19.4	11.4	4.7	3.3		15.4	9.1	3.9	2.4
day[c]		13.8	8.7	3.6	1.5		12.0	7.5	3.0	1.6		10.2	6.3	2.6	1.3
night[d]		10.5	5.6	2.6	2.4		7.4	4.0	1.7	1.7		5.3	2.8	1.3	1.1
HNO_3		131.7	77.8	57.6	-3.7		74.2	45.6	35.1	-6.5		45.8	29.2	25.6	-9.0
NO_y					24.1					16.6					7.6

[a]We define the boundary of Southeast US is 25-40° N, 100-75° W. All budget terms are in Gg N.

[b]$\sum PNs$ includes PAN, peroxymethacryloyl nitrate (MPAN), and a C5 hydroxy peroxyacyl nitrate (C5PAN1) produced by oxidation of ISN1.

[c]Alkyl nitrates produced from oxidation of isoprene and monoterpenes by OH.

[d]Alkyl nitrates produced from oxidation of isoprene and monoterpenes by NO_3.